Aus der Klinik und Poliklinik für Kinder- und Jugendpsychiatrie,
Psychosomatik und Psychotherapie
der Ludwig-Maximilians-Universität München
Direktor: Prof. Dr. med. Gerd Schulte-Körne

White and Gray Matter Microstructure in Children with Predisposition for Dyslexia – a Diffusion Tensor Magnetic Resonance Imaging Study

Dissertation
Zum Erwerb des Doktorgrades der Medizin
an der Medizinischen Fakultät der
Ludwig-Maximilians-Universität zu München

vorgelegt von
Paweł Piotr Wróbel
aus Bydgoszcz
2021

Mit Genehmigung der Medizinischen Fakultät
der Ludwig-Maximilians-Universität München

Berichterstatter:	Prof. Dr. med. Inga Katharina Koerte
Mitberichterstatter:	Prof. Dr. med. Franziska Dorn
	Prof. Dr. med. Marco Düring
	Prof. Dr. med. Thomas Meindl
Dekan:	Prof. Dr. med. Thomas Gudermann
Tag der mündlichen Prüfung:	23.12.2021

TABLE OF ABBREVIATIONS AND SYMBOLS 5
LIST OF FIGURES 6
EIDESSTATTLICHE VERSICHERUNG 9
1 SUMMARY 10
2 ZUSAMMENFASSUNG 11
3 INTRODUCTION 12

3.1 Characteristics of developmental dyslexia (DD) 12
3.1.1 Characteristics of deficits in DD 12

3.2 Pathology in light of cerebral maturation 14
3.2.1 Altered neuronal migration as a potential cause of structural brain alterations in DD 14
3.2.2 Genetic influence on dyslexia 15

3.3 Review of observed cerebral micro- and macrostructural alternations in magnetic resonance imaging (MRI) studies 17
3.3.1 Review of macrostructural morphometry in MRI studies in DD 23
3.3.2. Review of microstructural abnormalities in MRI studies of DD 24
3.3.3 Methodological considerations 25
3.3.4 Technical background on heterogeneity (HG) of diffusion measures 26

3.3 Outline of the hypothesis-driven approach 28

4 METHODS 31

4.1 Participants 31
4.1.1 Characteristics of the BOLD-study participants 31
4.1.2 Non-verbal neuropsychological items 32
4.1.3 Verbal neuropsychological items 32
4.1.4 Analyzed subgroups 33

4.2 MRI data analysis 34
4.2.1 Data acquisition 34
4.2.2 MRI data preprocessing 35

4.3 Obtaining HG measures 37
4.4 The Lateralization Index (LI) 38
4.5 Statistical analysis 39
4.5.1 Significance level and correction for multiple comparisons 40

5 RESULTS 41

5.1 HG assessment in FHD+ children and poor readers 41
5.1.1 Analysis A: HG in children with family history of DD 41
5.1.2 Analysis B: HG in poor readers 42
5.1.3 Analysis C: HG in poor FHD+ readers 43

5.2 Testing for the second hypothesis: HG in diffusion as a prognostic measure of reading performance 44
5.2.1 Analysis D: HG as a predictor for reading performance 44

6 DISCUSSION 46

6.1 HG in individuals at risk for DD and in impaired readers 46
6.1.1 Conclusions from the analysis of individuals at risk for DD 46

6.1.2 Conclusions from the analysis on poor readers 48
6.1.3 Conclusions from the analysis on poor readers at risk 48
6.1.4 Conclusion on heterogeneity and genetic risk for DD 48

6.2 HG as a predictor for future reading skills 49
6.3 Limitations 50
6.4 Future perspectives 50
6.5 Conclusion 52

7. SUPPLEMENTARY MATERIAL 53

7.1 Analysis A – HG and genetic risk for DD 53
7.2 Analysis B – HG and reading performance 55
7.3 Analysis C – HG and poor FHD+ readers 57
7.4 Analysis D – HG as predictor for performance 59

8 BIBLIOGRAPHY 61
9. ACKNOWLEDGEMENTS 70

Table of abbreviations and symbols

AF	arcuate fasciculus
ANCOVA	analysis of covariance
CTOPP	Comprehensive Test of Phonological Processing
DD	developmental dyslexia
DICOM	digital imaging and communications in medicine
dMRI	diffusion magnetic resonance imaging
DTI	diffusion tensor imaging
DWI	diffusion weighted imaging
fMRI	functional magnetic resonance imaging
EPI	Single-shot echo planar imaging
FA	fractional anisotropy
FHD+	positive family history of dyslexia
FHD-	negative family history of dyslexia, control group
GM	gray matter
HG	heterogeneity
HLE	Home Literacy Environment
IQ	intelligence quotient
KBIT	Kaufman Brief Intelligence Test
λ	tensor's eigenvalue
μ	mean
MD	mean diffusivity
MNI	Montreal Neurology Institute
MRI	magnetic resonance imaging
NIFTI	Neuroimaging Informatics Technology Initiative
NRRD	Nearly Raw Raster Data
PP	phonologic processing
ROI	region of interest
σ	Standard deviation
TOWRE	Test of Word Reading Efficiency
WM	white matter

List of figures

Figure 1	Simplified schematic model of reading networks	13
Figure 2	Schematic model of a healthy cortex and altered cortex in DD	15
Figure 3	Streamline of the workflow for heterogeneity estimation	27
Figure 4	Examples of motion artifacts in T1 and DWI	36
Figure 5	Cortical segmentation in native and DWI space based upon the Desikan-Atlas (Desikan et al., 2006)	37
Figure 6	Scatter plot depicting GM heterogeneity in relationship to age	42
Figure 7	Boxplot depicting left frontal WM heterogeneity differences in children risk for dyslexia	42
Figure 8	Boxplot depicting left frontal WM heterogeneity differences in children risk for dyslexia with worse reading performance	44
Figure 9	Scatter plot depicting correlation of left parietal GM heterogeneity with later rapid naming performance	45

List of tables

Table 1	Numbers of exclusions and inclusions in the review process	18
Table 2	Summary of findings on literature in T1 weighted imaging in developmental dyslexia	19
Table 3	Summary of findings on literature in diffusion MRI in developmental dyslexia	21
Table 4	Parameters of acquired DWI weighted images	34
Table 5	Parameters of acquired T1 weighted images	34
Table 6	Excluded and included DWI weighted images	35
Table 7	Excluded and included T1 data sets	35
Table 8	Demographic data in Analysis A	41
Table 9	Demographic data in Analysis B	43
Table 10	Demographic data in Analysis C	43
Table 11	Demographic data in Analysis D	45
Table 12	Heterogenetiy (HG) in gray matter (GM) of individuals at higher genetic risk for dyslexia	53
Table 13	Heterogenetiy (HG) in white matter (WM) of individuals at higher genetic risk for dyslexia	53
Table 14	Heterogeneity (HG) lateralization index (LI) in gray matter (GM) of individuals at higher genetic risk for dyslexia	54
Table 15	Heterogeneity (HG) lateralization index (LI) in white matter (WM) of individuals at higher genetic risk for dyslexia	54
Table 16	Heterogenetiy (HG) in gray matter (GM) of impaired readers	55
Table 17	Heterogenetiy (HG) in white matter (WM) of impaired readers	55
Table 18	Heterogeneity (HG) lateralization index (LI) in gray matter (GM) of impaired readers	56
Table 19	Heterogeneity (HG) lateralization index (LI) in white matter (GM) of impaired readers	56

Table 20 Heterogenetiy (HG) in gray matter (GM) of impaired readers at higher genetic risk for dyslexia 57
Table 21 Heterogenetiy (HG) in white matter (WM) of impaired readers at higher genetic risk for dyslexia 57
Table 22 Heterogeneity (HG) lateralization index (LI) in gray matter (GM) of impaired readers at higher genetic risk for dyslexia 58
Table 23 Heterogeneity (HG) lateralization index (LI) in white matter (WM) of impaired readers at higher genetic risk for dyslexia 58
Table 24 Heterogenetiy (HG) in gray matter (GM) as predictor for rapid naming and phonologic processing 59
Table 25 Heterogenetiy (HG) in white matter (WM) as predictor for rapid naming and phonologic processing 59
Table 26 Heterogeneity (HG) lateralization index (LI) in gray matter (GM) as predictor for rapid naming and phonologic processing 60
Table 27 Heterogeneity (HG) lateralization index (LI) in white matter (WM) as predictor for rapid naming and phonologic processing 60

Eidesstattliche Versicherung

Wróbel, Paweł Piotr
(Name, Vorname)

Ich erkläre hiermit an Eides statt, dass ich die vorliegende Dissertation mit dem Titel

White and Gray Matter Microstructure in Children with Predisposition for Dyslexia – a Diffusion Tensor Magnetic Resonance Imaging Study

selbstständig verfasst, mich außer der angegeben keiner weiteren Hilfsmittel bedient und alle Erkenntnisse, die aus dem Schrifttum ganz oder annähernd übernommen sind, als solche kenntlich gemacht und nach ihrer Herkunft unter Bezeichnung der Fundstelle einzeln nachgewiesen habe.

Ich erkläre des Weiteren, dass die hier vorgelegt Dissertation nicht in gleicher oder in ähnlicher Form bei einer anderen Stelle zur Erlangung eines akademischen Grades eingereicht wurde.

München, 27.12.2021	Wróbel, Paweł Piotr
Ort, Datum	Unterschrift Doktorand

1 Summary

With a prevalence of 5–17%, developmental dyslexia (DD) is the most common developmental disorder and leads to compromised quality of life. However, despite this high prevalence, its pathology is not entirely understood. Early post-mortem studies in DD showed abnormal histology of the cerebral cortex including cortical heterotopia and abnormal cortical gyration patterns. Later, the advent of magnetic resonance imaging (MRI) facilitated in-vivo investigations suggesting abnormal white matter (WM) microstructure and gray matter (GM) morphometry. These findings are in line with genetic mutations that have been identified in DD, which are associated with altered neuronal migration. In this work, a novel method, based on variability of measures derived from diffusion tensor imaging (DTI), called heterogeneity (HG), was used to shed light on GM and WM microstructure in individuals at risk for DD.

First, HG in the frontal, parietal and temporal lobes was examined for differences between controls and a) individuals with increased risk for DD, b) a group with low reading performance and c) a sub-group with both familiar risk and low performance. A prospective approach was used to explore whether HG is a suitable predictor of reading skills. The participants were children with a family history of DD and part of the Boston Longitudinal Study of Dyslexia. The study acquired behavioral and MRI data prior to the start of school as well as at annual follow-up sessions during the subsequent six years. The HG of diffusion was retrieved from diffusion weighted images.

There were no statistically significant findings in the analyses. The data revealed a tendency of higher WM HG in individuals at risk for DD at the cross-sectional level, which can potentially be driven by GM heterotopia. In the prospective approach, HG in the parietal cortex predicted later rapid naming skills, pointing toward a trend of cortical microstructure being associated with reading performance. Nevertheless, the unprecedented and intuitive results provide a valuable base for further investigations of the cerebral and in particular the cortical microstructure.

2 Zusammenfassung

Dyslexie ist mit einer Prävalenz von 5–17% die häufigste Entwicklungsstörung und führt zu starker Beeinträchtigung im Alltag. Die zugrunde liegende Pathologie bleibt nicht gänzlich geklärt. In post-mortem Studien konnten Heterotopien grauer Substanz, Veränderung von Gyrierungsmuster und Mikrostruktur des Cortex bei Patienten mit Dyslexie beobachtet werden. Mit der Etablierung der Magnetresonanztomographie (MRT) wurden in-vivo Untersuchungen zerebraler Struktur möglich. Diese weisen auf Veränderungen der Mikrostruktur der weißen Substanz, sowie auf Veränderungen der Volumina kortikaler Areale hin. Dies steht im Einklang mit genetischen Studien, in denen eine beeinträchtigte neuronale Migration als Auslöser für die veränderte Mikrostruktur postuliert wird. In dieser Arbeit wird eine neue Methode, die „Heterogenität“ von Diffusionsparametern genutzt, um die cortikale und subcortikale Mikrostruktur bei Kindern mit familiärem Risiko für Lese- und Rechtsschreibschwäche zu charakterisieren.

Die vorliegende Arbeit untersuchte zunächst Gruppenunterschiede in der Heterogenität in den Frontal-, Parietal- und Temporallappen. Außerdem wurde in einer Längsschnittstudie untersucht, ob die Heterogenität ein möglicher Prädiktor für spätere Lesefähigkeiten darstellt. Die hier ausgewerteten Datensätze entstammen der Boston Longitudinal Study of Dyslexia. Diese Studie untersuchte Kinder vor Schuleintritt und danach jährlich über einen Zeitraum von sechs Jahren. Es wurden Daten zur Lesefähigkeit sowie und MRT Daten erhoben. Die Heterogenität wurden basierend auf den diffusionsgewichteten MRT Sequenz berechnet. Die statistische Auswertung erfolgte in Untergruppen mit erhöhtem familiärem Risiko, mit schlechter Leseleistung sowie bei Individuen mit sowohl familiärem Risiko als auch schlechter Lesefähigkeit.

Es zeigten sich keine statistisch signifikanten Ergebnisse. Die Ergebnisse weisen jedoch auf Tendenzen erhöhter Heterogenität in der frontalen weißen Substanz bei Kindern mit familiärer DD hin. Die erhöhte Heterogenität könnte Ausdruck von subtiler Migrationsstörung der grauen Substanz sein. Die parietale kortikale Heterogenität zeigte eine Korrelation mit späterer Benenngeschwindigkeit und könnte auf einen Zusammenhang zwischen kortikaler Mikrostruktur und späterer Lesefähigkeit deuten. Die in dieser Arbeit berichteten Ergebnisse bilden eine wertvolle Basis für zukünftige Forschungsfragen zur Pathophysiologie der Lese-/Rechtschreibschwäche.

3 Introduction

3.1 Characteristics of developmental dyslexia (DD)

According to the World Health Organization (WHO), developmental dyslexia (DD) refers to a deficiency in text comprehension, word recognition and reading performance, as well as slower acquisition of these skills, which cannot be justified by insufficient training, poor sight or social status (WHO, 2014, Stanovich, 1996). The syndrome includes a broad spectrum of symptoms – individuals with DD may experience impairment in, for example, speech perception, rapid naming, phonologic awareness, auditory memory and, or orthographic knowledge (Schulte-Korne et al., 2006). With the prevalence of DD ranging from 5% to 17%, it is the most frequently observed developmental disorder (Shaywitz et al., 1998, Moll et al., 2014). DD is more prevalent in male individuals (reported ratio range: 1.2–6.78) but also assumed lower diagnostic sensitivity in female readers (Quinn and Wagner, 2015).

Reading plays a crucial role in the era of electronic media, with written text often being the main form of communication in private, professional, and public matters. DD compromises one's reading skills and thus, impairing functionality and quality of life (Nelson and Liebel, 2018). DD has been shown to be accompanied by comorbidities, including attention deficit hyperactivity disorder (ADHD) which is reported in 15% of cases and calculation deficits, which are reported in 40% of cases (Gooch et al., 2014, Moll et al., 2014). Moreover, individuals with DD are more likely to develop secondary psychiatric disorders such as depression and anxiety (Maag and Reid, 2006, Schulte-Korne et al., 2003, Nelson and Liebel, 2018). As the pathology of DD is not yet entirely understood, it remains a challenge to provide effective and efficient treatment.

3.1.1 Characteristics of deficits in DD

The behavioral deficits in DD have been discussed since the disorder's first description. Morgan made initial assumptions on "word blindness" and explained DD with sight insufficiency and abnormal vision areas in the brain (Morgan, 1896). Later hypotheses also focused on disruptions in the visual system (Hermann, 1959), oculomotor deficits (Getman, 1985) and a less efficient magnocellular system, which stabilizes images

during oculomotor action (Livingstone et al., 1991, Galaburda and Livingstone, 1993). Despite the plausibility of assumptions of the pathology in the visual system, today, they are no longer discussed as the central pathology in DD. In fact, unimpaired vision and recognition belong to DD's diagnostic criteria (Olulade et al., 2013).

In the neurobehavioral studies by Vellutino et al., the authors recognized and proposed that the model of DD should be extended by the linguistic network (Vellutino, 1979, Vellutino, 1987). The shift to understanding DD as a multilateral problem aligns with the modern understanding of the brain as a network rather than an aggregate of specialized subunits processing information one after the other (Griffa et al., 2013). As presented in the model in Figure 1, processing within the reading network can be simplified with a two-stream hypothesis, which is based on two parallel used pathways (Liebenthal et al., 2013).

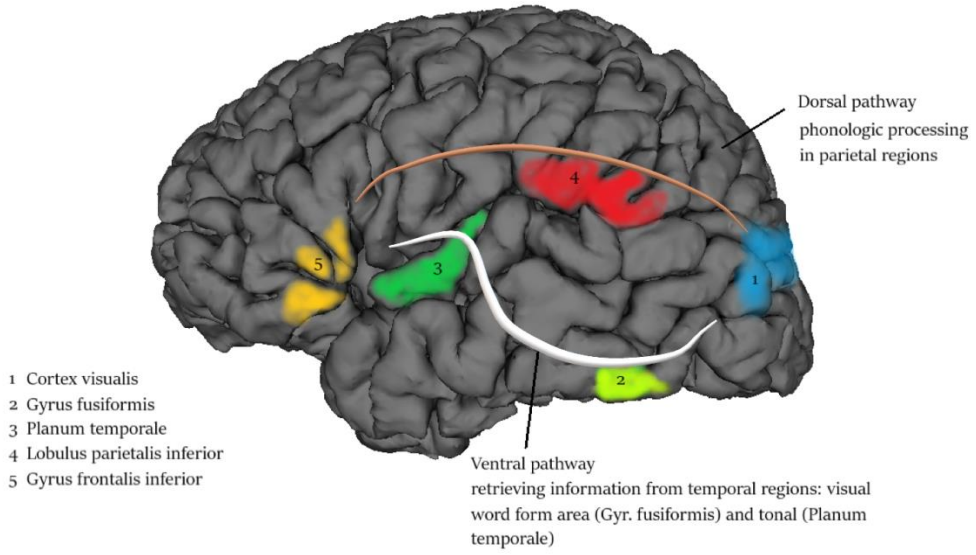

Figure 1 Simplified scheme of the reading network. The information from the visual system in the occipital cortex is either processed by the dorsal pathway (phonologic processing) or the information stored in the visual word form area and other temporal sources. Both streams lead to a synthesis in the frontal lobe, in particular the inferior frontal gyrus. Source: Own work.

The linguistic areas, which play the main role in Vellutino's assumptions, are located rostral to the visual area, in the fronto-temporo-parietal network. The dorsal pathway, which is highlighted as the brown stream in Figure 1, connects the occipital visual areas with parietal areas and the inferior frontal gyrus. The linkage to the parietal multisensory system contributes to data's appraisal and facilitates phonologic processing (Liebenthal et al., 2013, Hickok et al., 2011). Phonologic processing is responsible for coupling and modifying sounds as carriers of particular information. It is

necessary, for example, in the task of removing the phoneme “b” from the word “bold” to create the word “old”. Furthermore, it was shown to be compromised in individuals with DD and to correlate with imaging findings discussed in section 3.3 (Boets et al., 2013, Carroll et al., 2014, Yeatman et al., 2011, Vandermosten et al., 2012a).

The second pathway consists of the ventral stream, highlighted in white in Figure 1. This pathway connects the occipital and frontal lobe, through the temporal cortex. It is thought to facilitate the retrieval of sound information from the outward appearance of words from the fusiform gyrus (visual word form area [VWFA]) and audiological information from the planum temporale (Finn et al., 2014, Sigurdardottir et al., 2015). Rapid naming, which is a behavioral reading measure based on fast information retrieval, has been associated with abnormal function in the temporal lobe (Denckla, 1972, Denckla and Rudel, 1976, Raschle et al., 2011, Sigurdardottir et al., 2015). From a clinical perspective, in 1999, Wolf and Bowers divided DD into three forms in the “double-deficit” hypothesis. According to their work, individuals with DD display a deficit in phonologic processing, in naming speed or in both (Wolf and Bowers, 1999).

3.2 Pathology in light of cerebral maturation

3.2.1 Altered neuronal migration as a potential cause of structural brain alterations in DD

Autopsy studies in patients with DD point toward a disrupted macrostructure with scattered gray (GM) heterotopia in the white matter (WM), as well as volume asymmetry of the planum temporale (Galaburda and Kemper, 1979, Galaburda, 1993b, Galaburda, 1993a). On the microstructural level, Galaburda et al. found an abnormal structure of cortical layers as well as additional small gyri on top of the usual cortical gyri, the polymicrogyria (Galaburda and Kemper, 1979). These unusual findings provide a valuable starting point for considerations on potential pathology in DD.

A schematic model of abnormal cortical microstructure from post-mortem studies on cerebral structure is summarized in Figure 2.

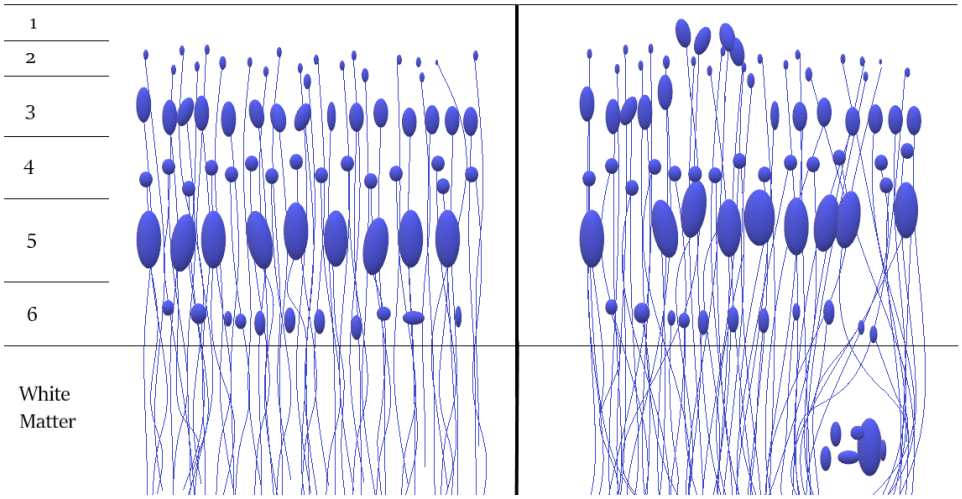

Figure 2 Schematic model of a healthy cortex (left) and altered cortex in DD (right)
The image on the left represents a model of healthy cerebral tissue, showing a relatively homogenous structure. On the right potential GM heterotopia in subcortical WM, as well as abnormally migrated cortical cells leading to microgyria (here symbolically indicated). 1 – stratum moleculare, 2 – external granular layer, 3 – external pyramidal layers, 4 – internal granular stratum, 5 – internal pyramidal stratum, 6 – multiform layer. Glial cells are not shown for simplicity purposes. Source: Author's own work.

Characteristics of brain structure develop early in utero by a process called neuronal migration (Clowry et al., 2010). Neurons migrate from the inner, ventricular zone to the outer pallial stratum guided by a scaffold made of radial glia cells (Campbell and Gotz, 2002). Wrongly migrating cells may not arrive at the cortex leading to heterotopia and/or cortical dysplasia (Krafnick et al., 2014, Wang et al., 2006). Neuronal migration is influenced by genetic factors which suggested a genetic connection to DD. In parallel, epidemiologic studies revealed that children, whose relatives have DD, have a higher risk (50–60%) of developing DD compared with children without positive family history (10%) (Hallgren, 1950, Grigorenko, 2001, Pennington and Lefly, 2001, Gallagher et al., 2000).

3.2.2 Genetic influence on dyslexia

After post-mortem brain examinations showed structural differences and epidemiological studies suggested hereditability, genetic studies were employed to examine the influence of genes on reading skills and cerebral structure. The first genetic analyses over three decades ago attempted to localize chromosome aberrations in DD (Smith et al., 1983). Until today, several candidate genes were identified and linked to mutations in dyslexia:

The proteins corresponding to the Doublecortin-Domain-Containing-Protein-2-Gene's (DCDC2) facilitate axonal growth and migration by interacting with the structure within the cytoskeleton (Bechstedt et al., 2014, Koizumi et al., 2006). Deuel et al. explained that a knockout in a murine model leads to callosal agenesis and alternated WM tracts (Deuel et al., 2006). Rodents with a single knockout exhibit less impairments than those with both alleles inactivated. Interestingly, diffusion tensor imaging (DTI) studies revealed higher fractional anisotropy (FA), a surrogate measure for axonal organization, in humans without deficiencies in the two DCDC2 alleles, whereas individuals with DCDC2 deficiencies had lower FA in the left hemisphere and corpus callosum (Marino et al., 2014).

Furthermore, the defects of KIAA0319 were observed in patients with DD and associated with supporting axonal growth and neuronal migration (Velayos-Baeza et al., 2007, Galaburda et al., 2006). Rodents with deactivated KIAA0319 presented worse responses to auditory stimuli (Centanni et al., 2014). In addition, imaging studies suggested that KIAA0319 genotype may be a predictor defining cortical thickness in the left orbitofrontal GM region and the FA in WM (Eicher et al., 2016).

Moreover, Dyslexia-Susceptibility-1-Candidate-1-Gene (DYX1C1 or DYX1) codes for a glial protein involved in neural migration (Rendall et al., 2015, Adler et al., 2013, Currier et al., 2011). Its absence is associated with disrupted migration (Carrion-Castillo et al., 2013). DYX1 interacts with other proteins, thus inducing activity of the above-mentioned DCDC2 (Tammimies et al., 2013). Temporoparietal WM volume and reading skills show positive associations with different genotypes of DYX1 (Darki et al., 2012).

Finally, Drosophila-Roundabout-Homolog-1-Gene (ROBO1) is linked with neuronal migration by regulating the axon guidance to its receptor domain (Moreno-Bravo et al., 2016). Its activation has been correlated with the linguistic processing and microstructure of the corpus callosum (Lamminmaki et al., 2012, Tran et al., 2014, Sun et al., 2017).

Disconnected-Interacting Protein 2 homolog A (DIP2A) was suggested to stimulate axonal growth and regulate synaptic plasticity (Mukhopadhyay et al., 2002). Poelmans et al. postulated that its mutation may be a factor for DD (Poelmans et al., 2009).

All of the five genetic mutations linked to DD (DCDC2, KIAA0319, DYX1, ROBO1 and DIP2A) have been shown to lead to abnormal neuronal migration. Since this type of migration is a basal mechanism, the resulting abnormal microstructure is likely to be widely spread. The observations on genetic mutations appear to be in line with the abnormal cerebral structure from autopsy studies (Galaburda and Kemper, 1979).

3.3 Review of observed cerebral micro- and macrostructural alternations in magnetic resonance imaging (MRI) studies

The assessments in the aforementioned autopsy studies have the limitation of few subjects, who are usually of high age. In contrast, imaging studies facilitate in-vivo and prospective investigations of brain structure even in child participants with DD. A variety of imaging studies have been conducted on the cerebral structure in DD. Due to the heterogeneous results on the micro- and macrostructure in reading disorders, considerations on the brain's morphology require a thorough review of the existing literature. Here, current literature on the micro- and macrostructure in DD was thus systematically gathered and summarized, and it is presented next. The review focused on original articles about individuals with a positive family history of DD (FHD+) and/or primary reading disorders. Exclusion criteria included: focus on secondary reading impairments (e.g. due to stroke) and focus different that the cerebral tissue research or descriptions of methodology.

The following qualitative review is based on standardized research applied to the PubMed database on November 22nd, 2020. Forty publications were identified for the item ("MRI" AND "white matter" AND "Dyslexia") and 34 on ("DTI" AND "white matter" AND "Dyslexia") in the title or abstract. Of the 74 hits, 11 were redundant, yielding a total of 63 publications. At the same time a search for articles on imaging of GM identified 21 publications on ("MRI" AND "gray matter" AND "Dyslexia"), 7 results on ("MRI" AND "grey matter" AND "Dyslexia"), 4 on ("DTI" AND "gray matter" AND "Dyslexia") and none on ("DTI" AND "grey matter" AND "Dyslexia"). Moreover, there were 10 duplicates, resulting in a total of 22 articles.

In total, 80 articles were identified on structural MRI findings in WM and GM. Later, 34 publications were excluded, as they focused on secondary reading impairments due to cerebral infarction, inflammatory disease, and epilepsy or on healthy individuals

without any clinical impairment. Three MRI studies did not examine the cerebral structure. On the other hand, three publications previously known to the author were included despite not appearing in the database search (Banfi et al., 2019, Su et al., 2018, Jednorog et al., 2014). A total of 46 articles were included in the review process and divided into two tables: Table 1 summarizes articles on microstructure in DD, and Table 2 lists articles on macrostructural findings in DD. Publications dealing with research into both, macro- and microstructure were attributed to the table on microstructure (Table 2).

	Items
Identified articles in data base research (redundant positions excluded)	80
Articles not identified in research but known to the author	3
Exclusion due to focus on secondary reading impairments	34
Exclusion due to being a methodological article	3
Total number of included publications	46
Included articles on T1 weighted imaging findings	20
Included articles on DWI findings	26

Table 2 Numbers of exclusions and inclusions in the review process.

First Author	Participants/Controls	Approach	Statistically significant findings
Dalby MA (Dalby et al., 1998)	17 DD+, 6 low performing readers, 12 controls	Voxel based whole brain volume analysis	Subcortical parainsular WM region with rightward asymmetry more prominent in dyslectic subjects.
Eliez S (Eliez et al., 2000)	16 DD+, 14 controls	Voxel based whole brain volume analysis	Decreased volume in temporal lobes, particularly in the left hemisphere and driven by GM volume.
Vinckenbosch E (Vinckenbosch et al., 2005)	10 DD+, 14 controls	ROI based GM analysis	Decreased GM volume in both temporal lobes and increased GM volume in both precentral gyri in DD+.
Laycock SK (Laycock et al., 2008)	10 DD+, 11 controls	Voxel based whole brain volume analysis	Only WM volume significantly higher in both cerebellar hemispheres in controls.
Pernet CR (Pernet et al., 2009)	38 DD+, 29 controls	Whole brain volume analysis	Areas discriminating subjects with dyslexia: rh cerebellar declive (6 voxels) and the rh lentiform nucleus (7 voxels).
Casanova MF (Casanova et al., 2010)	15 DD+, 11 controls	Gyral white matter depth analysis	DD+ had a deeper gyral WM than controls. Therefore, thicker cortices were proposed as inefficient.
Welcome SE (Welcome et al., 2011)	12 poor readers, 22 controls, 21 with compensated deficit	Radial expansion and thickness analysis	Left temporo-parietal volume asymmetry is higher in proficient readers. Higher thickness in lh medial occipital in readers with compensated reading abilities
Richardson FM (Richardson et al., 2011)	40 DD+, 34 controls	Voxel based density measurement	GM density in lh sup. temporal region is correlated positively with forward and backward digit span.
Krafnick AJ (Krafnick et al., 2014)	15 DD+, 15 age matched controls, 15 reading level matched controls (younger)	Voxel based whole brain volume analysis	GM volume: DD+< age matched controls: lh: middle temporal and cingulate gyrus. Rh: precentral, middle frontal and superior temporal gyrus |DD+<reading matched controls: rh precentral gyrus | DD+> reading matched controls: middle temporal gyrus WM volume: DD+< age matched controls: lh paracentral, middle frontal, middle frontal, superior frontal; rh middle frontal, precentral, deep temporal and anterior parathalamic |DD+> reading matched controls: right paraputaminal
Im K (Im et al., 2016)	28 DD+, 31 controls	Evaluation of sulcal patterns	Lh parieto-temporal and occipito-temporal sulcal patterns were significantly different in FHD+ and correlated with reduced performance in single word reading.
Ma Y (Ma et al., 2015)	32 DD+, 32 controls	ROI based whole brain thickness analysis	DD+ showed stronger rightward lateralization of thickness in the superior temporal gyrus.
Tamboer P (Tamboer et al., 2015)	37 DD+, 57 controls	Voxel based whole brain volume analysis	Rhyming skills correlated with GM volume in the lh and rh caudate nucleus and negatively with increased total WM volume
Xia Z (Xia et al., 2016)	24 DD+, 24 controls	Voxel based ROI volume analysis	Decreased GM volume in DD+: lh frontal, parietal, temporal and occipital lobes, bihemispherial precuneus, rh median cingulate and paracingulate gyri, rh occipital lobe, CC.
Tamboer P (Tamboer et al., 2016)	22 DD+, 27 controls	Voxel based whole brain (Machine learning on volume)	Lh inferior parietal gyrus and lh and rh fusiform gyrus volumes predicted DD.

Continued on the next page

First Author	Participants/Controls	Approach	Statistically significant findings
Kraft I (Kraft et al., 2016)	28 FHD+, controls	Quantification of T1 hyperintensities	FHD+<FHD-: lh anterior AF.
Phan TV (Phan et al., 2018)	13 DD+, 21 controls	Voxel based whole brain volume analysis	Tendencies in DD+ to lower have overall lower lh GM volumes.
Van Oers (van Oers et al., 2018)	26 DD+, 25 controls	Cerebellar volume analysis	No differences in local GM volume and no linkage of diffusion characteristics to performance at cerebellar level.
Jagger-Rickels AC (Jagger-Rickels et al., 2018)	41 ADHD+, 17 DD+, 16 ADHD+DD+, 32 controls	Volume analysis by subtraction of averaged maps	DD+<controls: in bilateral calcarine and lingual gyri, bilateral insulae, lh caudate nucleus, lh precentral gyrus, rh superior frontal gyrus and right anterior caudate nucleus.
Beaulieu C (Beaulieu et al., 2020)	20 DD+	Myelin Water Fraction (T2) derived	Myelin water fraction was observed to be higher in Corpus callosum, lh internal capsule and lh+rh thalamus.
Jednorog(Jednorog et al., 2014)	46 DD+, 35 controls	Voxel based whole brain volume analysis	GM volume was decreased in the lh inferior frontal gyrus.

Table 2 Summary of findings on literature from T1 weighted imaging in developmental dyslexia. WM: white matter. GM: gray matter. FHD: family history of dyslexia, lh: left hemispheric, rh: right hemispheric, DD+ diagnosed with dyslexia.

First Author	Cohort sizes	Approach	Statistically significant findings
Klingberg T (Klingberg et al., 2000)	6 DD+, 11 controls	Whole brain analysis on FA in WM	Bilateral WM in the temporo-parietal region.
Deutsch GK (Deutsch et al., 2005)	7 DD+, 7 controls	Whole brain WM analysis	FA higher in controls in a cluster of 14 voxels in the lh temporo-parietal region.
Richards T (Richards et al., 2008)	14 DD+, 7 constrols	Whole brain WM analysis (TBSS)	FA higher in 28 ROIs in controls: bilateral: pre-/postcentral, fusiform, superior occipital, parietal inf., and temporal inferior gyrus. Left hemisphere: frontal inf., lingual sup and sup. Temporal gyrus, precuneus, putamen, temporal sup. Right hemisphere: frontal sup. + med. + inf., suppl. Mot. Area, cuneus, medial occipital
Steinbrink C (Steinbrink et al., 2008)	8 DD+, 8 controls	Whole brain WM analysis + density in GM	FA in WM: FA higher in controls: left hemisphere: White matter caps. Externa and WM close to Gyr. Front. Inf., temp. sup., and occ. Med. Right hemisphere: insular WM. GM density: lower density in medial and superial temporal gyrus
Carter JC (Carter et al., 2009)	7 DD+, 6 controls	Tract ROI focused FA analysis	No differences in FA, only trend DD+<controls in right SLF.
Odegard TN (Odegard et al., 2009)	17 DD+, 7 controls	Whole brain WM analysis	DD+: Positive correlations with FA in the lh superior corona radiata and rh IFOF, rh UF, rh ILF, negative in CC
Rimrodt SL (Rimrodt et al., 2010)	14 DD+, 19 controls	Whole brain WM analysis	DD+: decreased FA in lh inferior frontal gyrus, lh insular WM and rh inferior frontal WM.
Keller TA (Keller and Just, 2009)	47 DD+, 25 controls	Whole brain WM analysis (intervention study)	FA increase after intensive reading training differences in phonological decoding positively correlated to FA, strongly negatively related to radial diffusivity
Hoeft F (Hoeft et al., 2011)	25 DD+, 20 controls	Tract based WM analysis (additionally fMRI)	FA in lh SLF correlated positively with word reading in controls but not in DD+.
Gebauer D (Gebauer et al., 2012)	42 with impaired spelling, 11 controls	Voxel based WM analysis (additionally fMRI)	FA higher in the lh anterior superior corona radiata (SCR) and anterior CC of controls.
Vandermosten M (Vandermosten et al., 2013)	20 DD+, 20 controls	Tractography study (FA)	FA decreased in DD+: lh: SLF, AF, ILF, Radiatio optica, CC, cerebellar peduncle, rh: SLF, CC.
Marino C (Marino et al., 2014)	20 DD+ (10 with DSDS2d mutation), 26 controls (10 with DSDS2s mutation)	Tractography study (FA)	DD+<controls: lower FA in the lh AF and CC (splenium)
Vandermosten M (Vandermosten et al., 2015)	36 FHD+, 35 FHD-	Tractography study (FA)	FA in lh AF correlated with phonological awareness in controls.
Richards TL (Richards et al., 2015)	17 DD+, 14 with dysgraphia, 9 controls	DTI: FA, RD AND AD + Tractography	DD+: lower FA in lh+rh anterior thalamic radiation, lh cingulum and forceps minor, AD: lh+rh CST bds, rh anterior thalamic radiation, rh cingulum, rh IFOF, rh SLF, rh UF. RD: lh CST, lh IFOF, lh ILF, lh SLF, lh UF, lf SLF.

Continued on the next page

First Author	Participants/Controls	Approach	Statistically significant findings
Fernandez VG (Fernandez et al., 2015)	29 DD+, 27 controls	Tractography study (FA)	FA was higher in DD+ in tracts connecting the cerebellum with temporoparietal and frontal regions.
Cui Z (Cui et al., 2016)	28 DD+, 33 controls	DTI + structural: WM volume and diffusion metrics in whole brain analysis	Diagnostic characteristics of 1) WM Volume: Sensitivity= 64.29%, Specificity= 75.76%, 2) FA: Sensitivity= 57.14%, Specificity= 66.67%, 3) MD Sensitivity= 57.14%, Specificity= 51.52%, 4) AD Sensitivity= 71.43%, Specificity= 72.73%, 5) RD Sensitivity= 39.29%, Specificity= 69.70%.
Richards TL (Richards et al., 2017)	20 DD+, 10 with dysgraphia, 6 with grammar impairment, 6 controls	Whole brain analysis	After training DD+ showed increase in RD: anterior corona radiata + superior frontal WM. AD: superior corona radiata, superior frontal WM, middle frontal WM and SLF. For MD: same as AD and additionally anterior coronal radiata.
Vanderauwera J (Vanderauwera et al., 2017)	15 DD+, 46 controls	Tractography (FA) restricted to AF as ROI	FA in left AF was a predictor for DD.
Wang HS (Wang et al., 2019)	24 DD+, 22 controls	Tract based whole brain analysis	Chinese character recognition correlates with the FA in IFOF, anterior CC as well as cerebellar and thalamopontine pathways.
Vanderauwera J (Vanderauwera et al., 2019)	35 DD+	Tractography study	FA in parts of left AF and UF correlates with word reading in DD+.
El-Sady S (El-Sady et al., 2020)	20 DD+	Voxel based whole brain study FA and ADC	FA reduction of right AF in DD+ correlates with worse overall reading skills. The ADC of right SLF is negatively correlated with memory abilities. The ADC of right internal capsule correlates positively with writing performance.
Zuk J (Zuk et al., 2020)	35 FHD+ and 39 FHD-	Tractography study	FA in the posterior right SLF was a predictor for dyslexia in children at risk
Vander Stappen C (Vander Stappen et al., 2020)	18 DD+ (trained), 13 DD+ untrained	ROI analysis of FA in AF as ROI	Reading training correlated with FA increase in AF.
Partanen M (Partanen et al., 2020)	13 DD+, 22 controls	DTI in WM and GM surface, thickness and volume	Better reading scores correlated with lower MD in rh insula and thinner cortex in lh fusiform gyrus, lh supramarginal gyrus, and bilateral supramarginal and inferior frontal gyri.
Banfi (Banfi et al., 2019)	20 DD+, 27 controls	Automated Fiber Quantification	DD+: higher FA in bilateral ILF, rh SLF and rh cingulum. Spelling deficits contributed to lower FA in lh AF compared to controls.
Su (Su et al., 2018)	18 DD+, 22 controls	Tractography study	DD+<controls: lh AF, lh ILF. The FA of the lh AF correlated with phoneme deletion, RAN and digit recall.

Table 3 Summary of findings on literature from diffusion MRI in developmental dyslexia. AD: axial diffusivity, FA: fractional anisotropy, MD: mean diffusivity, RD radial diffusivity WM/GM: white/gray matter. FHD: family history of dyslexia. RAN: rapid automatized naming, lh: left hemisphere, rh: right hemisphere, AF: Arcuate fascicicle, CC: corpus callosum, ILF: inferior longitudinal fascicle, SLF: superior longitudinal fascicle, CST:.corticospinal tract, IFG: Inferior frontal gyrus, ROI: region of interest.

3.3.1 Review of macrostructural morphometry in MRI studies in DD

According to voxel-based morphometry studies, individuals with DD are more likely to display an abnormal cerebral structure, especially in the form of decreased cortical volume, as presented in the tabular summary (Table 2). There is high variability in the localization of the observed alterations. Strikingly, the frontal, temporal and parietal lobes often seem to be impaired in DD (Eliez et al., 2000, Vinckenbosch et al., 2005, Jednorog et al., 2014, Xia et al., 2016). Right hemispheric GM appears to have a higher volume and thickness in DD, which leads to a rightward lateralization. The right hemisphere is thus considered either to show compensatory mechanisms or to simply be less susceptible to structural deficits (Ma et al., 2015).
In contrast to findings on telencephalic GM, a study identified the volume of GM in cerebellar declive and basal ganglia as a discriminator between participants with DD and healthy controls (Pernet et al., 2009). Discrepancies in localization and in the extent of findings also appear on the meta-analytic level. According to Eckert et al., left hemispheric frontal and temporal regions exhibit decreased GM volume in DD, whereas Richlan et al. identified bilateral superior temporal GM volume reduction, not observing any frontal abnormalities (Richlan et al., 2013, Eckert et al., 2016). A third meta-analysis found reduced left hemispheric GM volume in the fusiform gyrus and bilateral supramarginal and cerebellar cortices (Linkersdorfer et al., 2015). Similarly, the results on WM volume range from rightward asymmetry in parainsular WM to widespread, frontal volume deficits in individuals with DD (Krafnick et al., 2014, Dalby et al., 1998).

The review of cortical thickness seems to be similarly difficult, with discrepancies in the observed extent of observation. For example, Ma et al. postulate rightward lateralization to be associated with DD, whereas Welcome et al. observed a higher asymmetry in proficient readers (Ma et al., 2015, Welcome et al., 2011). The number of publications on cortical thickness is substantially lower than the number of articles on cortical volume. According to the author's knowledge, no meta-analyses exist.

Another question that must be addressed pertains to the comparability of findings on volume and thickness. Despite both being geometric measures, they must not be used interchangeably. Volume, which also depends on surface, was shown to have a higher variability and genetic dependence than thickness, and it is therefore a different measure

(Winkler et al., 2010). Furthermore, to date, it remains unclear whether less volume is associated with higher performance due to higher efficiency or whether a higher volume leads to higher performance due to the higher number of neurons (Walhovd et al., 2017, Tamnes et al., 2010).

In conclusion, there is much inconsistency in studies using different techniques and cohorts and presenting different extents of observed volume alterations in DD, ranging from bi-hemispherical lobar to small cerebellar regions (Vinckenbosch et al., 2005, Pernet et al., 2009). Despite the high variability, most original articles report findings in the frontal, temporal or parietal lobes. The accumulation of observations in this network in DD intuitively offers a point of origin for further studies on possible microstructural correlates. These, as mentioned above, can be caused by genetic mutations.

3.3.2. Review of microstructural abnormalities in MRI studies of DD

DTI examines the movement of water particles as a surrogate parameter for the tissue's microstructure (Basser and Pierpaoli, 1996). DTI studies have repeatedly shown that FA, which is an indicator for fiber organization, correlates with reading performance in temporal and parietal WM, especially in the arcuate fasciculus (AF) (Klingberg et al., 2000, Banfi et al., 2019, Vandermosten et al., 2012a). This seems plausible, since the AF connects the temporal and frontal speech areas. However, there are contradictory results, which do not state any differences in FA of the AF (Odegard et al., 2009). Some authors did not observe any statistically significant differences in individuals with DD at all (Carter et al., 2009). Similar to heterogeneous findings on macrostructure, the variety of techniques and cohort sizes in DTI studies on DD is wide (Table 3). The negative finding by Carter et al. may rely on small cohort sizes and insufficient statistical power. The results from meta-analyses summarizing the DTI findings are also inconsistent. These range from an absence of significant differences to clusters with decreased FA in frontal and temporal WM (Vandermosten et al., 2012b, Moreau et al., 2018).

In conclusion, findings on altered DTI measures in individuals with DD are dissimilar. However, the majority of articles seems to identify a decrease in FA in long tracts connecting the frontal lobe to the parietal and temporal regions. Thus, individuals with DD appear to show a higher fiber disorganization. These alterations in WM connections

are consistent with results from behavioral studies, suggesting impaired information retrieval with a sufficient amount of stored information (Ramus and Szenkovits, 2008).

Interestingly, to date, there are no published studies focusing on DTI of GM in DD. The four identified articles discussed findings based on DTI techniques in WM, but not in GM. It remains unclear whether structural cortical abnormalities in DD have any DTI correlates. Such an assumption remains intuitive in light of genetic studies suggesting that mutations contribute to altered migration and in light of histological findings of cortical dysplasia. This work hence aims to address microstructural alterations of GM in DD using diffusion MRI for the first time. Potential results may improve the understanding of the etiopathology of DD.

3.3.3 Methodological considerations

Magnetic resonance imaging (MRI) is based on the fact that the precession of an atom's spin is susceptible to magnetic field (Haacke, 1999). A magnetic energy pulse forces the precession in a certain direction. After the pulse, the atoms return to their initial state, which emits energy, registered as a signal and reconstructed into a virtual image. Using this phenomenon, Basser and Pierpaoli described a technique to assess the behavior of water diffusion, caused by Brownian motion within brain tissue (Basser and Pierpaoli, 1996). The data is commonly measured via a single-shot echo planar imaging (EPI) sequence (Mori, 2007). A 90° pulse aligns all atoms' spins in one plane. Later, a magnetic field gradient is introduced to diphase particles, depending on their location, and a subsequent inverse pulse to rephrase (Mori, 2007). All particles will precess with the same frequency again, if they did not change their location. However, if their location changed, then their frequency would also change, causing a weaker signal. If this phenomenon is measured for both directions of three perpendicular axes in a three-dimensional model, the data can be reconstructed to a tensor. Thus, a tensor describes the water diffusion in a three-dimensional imaging unit, a voxel. The eigenvectors and eigenvalues of the tenor are the direction and diffusion in a particular direction (Basser and Pierpaoli, 1998).

The tensor has a shape depending on the characterized tissue. It is spherical or isotropic if diffusion is not restricted. In WM, hydrophobic myelin sheaths rich in phospholipids prevent water movement perpendicular to the tract's direction. Therefore, the diffusion

is more likely to take place along the axons, and the tensor appears to be more anisotropic. Its form becomes comparable to a cigar.

The surrogate parameter of probability for directed diffusion along the main axis is quantified by FA, a ratio value, ranging from 0 to 1. It has lower values in media with more isotropic diffusion patterns (e.g. GM), and higher values in tissue with diffusion barriers, such as neurites in WM. FA is being calculated from the tensor's eigenvalues:

$$FA = \sqrt{\frac{3}{2}} \frac{\sqrt{(\lambda_1 - \mu\lambda)^2 + (\lambda_2 - \mu\lambda)^2 + (\lambda_3 + \mu\lambda)^2}}{\sqrt{\lambda_1{}^2 + \lambda_2{}^2 + \lambda_3{}^2}}$$

where λ_1, λ_2 and λ_3 are eigenvalues and $\mu\lambda$ is their mean (Basser and Pierpaoli, 2011).

Radial, axial and mean diffusivity are three diffusion measures frequently used along FA. Axial diffusivity (AD), represents the diffusion along the tensor's main axis (AD= λ_1). Radial diffusivity (RD) represents the mean of perpendicular diffusivity to AD (RD= $(\lambda_2 + \lambda_3)/2$). Mean diffusivity (MD) is the sum of all eigenvalues (MD= $(\lambda_1 + \lambda_2 + \lambda_3)/3$) (Mori, 2007). AD is thought to represent axonal organization and size and RD is postulated to evaluate differences in myelination (Song et al., 2002, Frye et al., 2011).

3.3.4 Technical background on heterogeneity (HG) of diffusion measures

Fiber-rich, hydrophobic structures such as axons in WM increase the probability of water diffusion along these structures and restrict it in perpendicular direction, resulting in high FA values. The cortical GM has different architectonics and consists of six differently built layers (Nolte, 2009). In contrast to the axons in WM, somas of neurons and synapto-dendritic connections do not force the diffusion along a certain direction (Basser et al., 2000). Therefore, FA is a less suitable parameter for GM organization compared to WM. Different approaches are hence needed to interpret measures derived from dMRI (McKinstry et al., 2002).

Heterogeneity (HG) is a newly established measure used to assess the variability of diffusion measures within a given region of interest (Rathi et al., 2014). A tissue with similar diffusion patterns across all voxels will display a lower HG as a sign of being uniform in microstructure. In contrast, a tissue with highly varying diffusion patterns between voxels will display a higher HG, indicating a diverse microstructure, which is suspected in DD. According to Rathi et al., the variability might be different between

two subjects even though the mean remains similar. In this case, scattered alterations such as disturbances in the six-layer architecture or local fluctuations in synaptic density, could influence the variability more than the overall FA. HG has been shown to positively correlate with age suggesting an increase in diffusion variability in the aging model (Rathi et al., 2014). It is calculated from diffusion measures within predefined regions obtained from segmentation of T1-weighted images. The streamline is schematically outlined below, in Figure 3. HG is expected to identify differences in variability of a diffusion measure within a region-of-interest with higher sensitivity compared to using the mean of a diffusion measure. Since small-sized abnormalities distributed across wide regions are expected in DD, HG appears to be a suitable technique for investigations in DD.

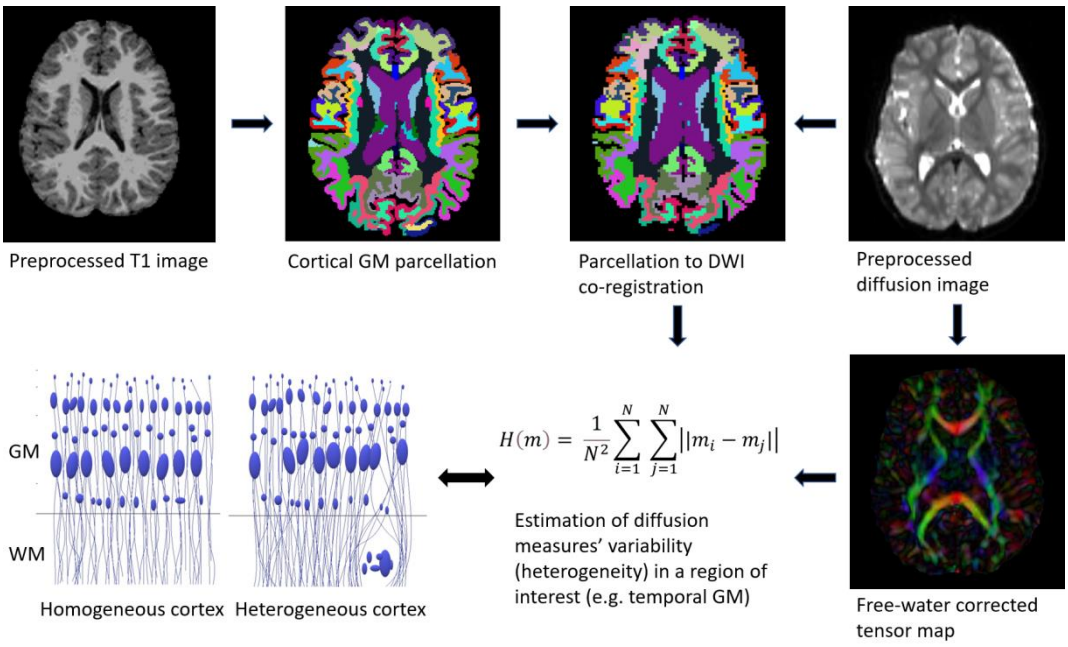

Figure 3 – Workflow for heterogeneity (HG) estimation. Based on the description by Rathi et al. and Seitz et al. (Rathi et al., 2014, Seitz et al., 2018).
Preprocessed diffusion and structural imaging data sets are used for the method. The structural T1 image is segmented and parcellated with subsequent registration on the DTI image. After correction for free-water a tensor map is estimated from the DWI data. Subsequently the variability of diffusion measures within an ROI from the parcellation is calculated. A cortex with varying space for diffusion will therefore show a higher HG. A homogeneous cortex will display lower HG. Source: Author's own work.

3.3 Outline of the hypothesis-driven approach

DD is associated with WM alterations (as assessed using DTI), cortical dysplasia (as assessed using post-mortem histopathological examination) as well as with genetic mutations linked to neuronal migration. Yet, to date, it remains unknown, if DD is associated with alterations of cortical microstructure and whether those can be assessed using DTI. HG, an established measure for the variability of diffusion measures, will be used to examine the relationship between genetic risk for dyslexia and the microstructure of both GM and WM in pre-school children (Rathi et al., 2014).

Testing will be conducted in children with phenotypic risk, i.e., impaired reading skills, children with genetic risk, i.e., positive family history of DD (FHD+) and an age-matched normally developing control group. Evaluating the influence of genetic factors is crucial to understanding of DD as a diagnosis, with a specific pathologic mechanism rooted in genetic mutations. From a neuro-psychiatric point of view, DD is not one entity but rather a spectrum of disorder. However, only a minority of original articles in the review (section 3.3) focused on potential genetic pathology and not solely on reading skills. This work offers a unique approach and synoptic analysis of a group at higher genetic risk, a group with poor reading performance, as well as a combination of both genetic and phenotypic risk.

The key regions of this work are the frontal, parietal and temporal lobes. As demonstrated in the review on imaging findings in DD, these regions have recurrently displayed lateralized macro- and microstructural abnormalities, correlating with behavioral measures.

Based on the existing gap in understanding of the brain's microstructure in DD, this work is based on two main hypotheses:

1. FHD+ individuals exhibit increased HG of diffusion due to mutations causing altered GM and WM microstructure, especially in the left hemisphere. Three analyses will be used to characterize the connection between genetic risk and HG.

A In the first analysis (Analysis A), the relationship between HG and genetic risk status will be tested. DD has high inheritance rates. Several genetic mutations in DD have been found to lead to abnormal GM and WM structure through impaired neuronal migration. A higher HG compared to the control group will support the hypothesis of DD as a genetic disorder.

B The second analysis (Analysis B) assesses the relationship between HG and reading performance, independent from genetic risk. The results will not only provide a statement on the linkage between function and the form of GM and WM, but will also facilitate interpretation of analysis A.

There are four possible outcome combinations of Analyses A and B. HG measures may or may be not linked with both, genetic risk and reading performance. First, two significant findings may imply, but not prove, that genetic risk leads to changes in microstructure and influences later reading skills. Furthermore, there could be a constellation with only one positive finding. For example, a negative finding on HG and reading performance and a positive one on HG and genetic risk. This would suggest that genetic mutations have an influence on microstructure, without later influencing reading skills. On the other hand, a link between microstructure and function but not with genetic risk, would suggest that the form is related to the function and widely independent of genetic mutations.

C The third analysis (Analysis C) supplements Analyses A and B. HG will be compared between a subgroup of FHD+ individuals who also show poor reading performance and healthy controls. A positive finding would indicate that children with both, genetic risk and poor reading performance display an abnormal structure. However, a positive finding exclusively in Analysis C would suggest only an effect in symptomatic FHD+ children and thus a strong influence of mutations on reading status. Furthermore, in light of a potentially negative finding in Analysis B, a finding in Analysis C would suggest HG as a valid diagnostic criterion.

2. HG at pre-school age (before learning to read) predicts future rapid naming and phonologic processing skills.

D Analysis D will evaluate whether or not HG of FA and MD in GM and WM, as well as its lateralization, predict future reading skills. HG measures of children at pre-school-age, prior to receiving reading training, may be a potential predictor for later reading skills at follow-up sessions (after at least two years of reading education). Rapid naming and phonologic processing have been chosen for the testing due to the considered link to specific brain areas. Existing studies postulate rapid naming to activate primarily temporal areas and phonologic processing parietal areas (Centanni et al., 2019, Liebenthal et al., 2013).

4 Methods

Data analyzed in this work is part of the Boston Longitudinal Study of Dyslexia (the BOLD study), Principal Investigator Dr. Nadine Gaab, funded by the National Institutes of Health, USA. After approval by the Institutional Review Board of Boston Children's Hospital (IRB Protocol Number: IRB-P00000284), written informed consent was obtained from participants' legal guardians, and verbal assent from the participants themselves according to the Declaration of Helsinki. The BOLD study addresses risk factors and predictors for DD in pre-school children with positive family history for DD using MRI.

4.1 Participants

4.1.1 Characteristics of the BOLD-study participants

Between September 11th 2008 and July 7th 2018, the research team – led by Dr. Gaab from Boston Children's Hospital – acquired demographic and reading performance data, as well as MRI images. In total, 109 (59 male and 50 female) natively English-speaking children from the Greater Boston Area participated in the study. The initial imaging and behavioral testing took place prior to primary education and reading training (pre-school age). Follow-up imaging and testing sessions were performed annually in the subsequent seven years. In total 342 T1-weighted and 244 DWI data sets were obtained.

Participants were recruited by pamphlet information in kindergartens and assigned either to the group of participants with FHD+, if having at least one first-degree relative with DD, or to a control group (FHD-), if none of the first-degree relatives had DD. During the study, 15 FHD- participants reported possible DD in non-first-degree relatives, which led to the creation of a subgroup with unclear risk (other [OTH]). Exclusion criteria consisted of former history of head trauma, neurological or psychiatric disorders, psycho-pharmacological treatment, preterm birth and problems with hearing or vision that cannot be corrected. One participant had a non-verbal intelligence quotient (IQ) below 85, which is a score below the first standard deviation, and was therefore excluded. In total, there were 47 FHD+, 47 FHD- and 15 OTH participants.

4.1.2 Non-verbal neuropsychological items

Non-verbal IQ was assessed using the second edition of the Kaufman Brief Intelligence Test (KBIT) (Kaufman, 2014). The KBIT is a standardized score with an average IQ equal to 100 and a standard deviation of 15 indicating the normal range. IQ was assessed to ensure comparability between groups and to account for the potential impact on reading skills.

Furthermore, previous studies have shown correlations between interaction with literature at home and reading performance (Storch and Whitehurst, 2001, Evans et al., 2000, Roberts et al., 2005). The Home Literacy Environment index (HLE) was thus included to control for influence of additional reading training at home. This surrogate parameter for contact to reading in everyday life is composed of items such as the number of books at home, time invested in reading, time invested in listening to a reading person or creative text production.

4.1.3 Verbal neuropsychological items

Established testing instruments were selected to assess reading skills. The following tests were performed at each time point unless indicated otherwise.

The Rapid Automatized Naming Test (RAN) (Wolf, 2005, Wolf and Bowers, 2000) is based on naming pictures or words presented to the participant in the shortest possible time (Denckla and Rudel, 1976). RAN is expressed as a score with a mean of 100 and a standard deviation of 15. At baseline examination (pre-school), RAN was performed by presenting pictures only, and no words were presented to the participant, as RAN for printed words requires a minimum of reading training.

Phonological competence was tested with the Comprehensive Test of Phonological Processing (CTOPP) (Rashotte, 1999). The test is based on elision performance, which is the skill to remove phonological information in spoken words in order to create other words. For example, removing the first phoneme in the word “bold” will result in the word “old”. The standardized mean is 10 and the range of first standard deviation is 3.

The testing battery in the BOLD study also covered the Test of Word Reading Efficiency (TOWRE), the Clinical Evaluation of Language Fundamentals and the

Woodcock Reading Mastery Test (WRMT) (Torgensen et al., 1999, Howard and Hulit, 1992, Woodcock, 1998). Tests operationalizing the entire process of reading are linked to function of multiple brain areas as indicated in subchapter 3.1.1. In contrast, tests linked to particular sub-functions used in reading will more likely facilitate connecting particular deficits in reading to specific cortical areas. Due to the hypothesized link of HG and basal components of reading as well as the existing evidence from the BOLD study, the focus was primarily laid upon RAN and CTOPP measures (Raschle et al., 2014). Furthermore, including TOWRE and WRMT for additional exploratory purposes would decrease the number of degrees of freedom in the statistic evaluation leading to less reliable statistical models.

4.1.4 Analyzed subgroups

4.1.4.1 Analysis A: different risk status for DD

The groups in Analysis A consist of FHD+ children with at least one first-degree relative with DD and FHD- controls. All children received at least two years of education in reading at school and had a non-verbal IQ of at least 85.

4.1.4.2 Analysis B: different reading performance

"Poor readers" were defined as individuals with at least one year of reading education and a score below the first standard deviation in RAN or CTOPP (≤7 for CTOPP and ≤85 for RAN). Controls had scores ≥10 for CTOPP and ≥105 for RAN. These cut-offs were chosen to discriminate poor readers from good readers.

Since the groups in this analysis were based on the phenotype of reading performance and not genetic risk status, the OTH group was included as well.

4.1.4.3 Analysis C: combined phenotype and family risk for dyslexia

A cross-sectional comparison was performed between poorly performing FHD+ individuals and well-reading FHD- controls. Cut-offs for neurobehavioral testing scores were as described for Analysis B.

4.1.4.4 Analysis D: association of HG and later reading skills

In order to examine whether the cerebral structure is related to later reading outcomes (RAN and CTOPP) after at least two years of reading training, all baseline datasets with available T1-weighted and DWI imaging were considered.

4.2 MRI data analysis

4.2.1 Data acquisition

Image sequences for all participants were acquired on a 3.0 Tesla Trio Tim Scanner (Siemens Medical Solutions, Erlangen, Germany) at Boston Children's Hospital in Waltham, Massachusetts, USA. An EPI sequence was used to gather DWI data, and multi-echo magnetization-prepared rapid gradient-echo (MEMPRAGE) was used for acquisition of high-resolution T1-weighted imaging. The parameters are listed in Tables 3 and 4. All participants underwent image acquisition on the same scanner with the same software version (B17). Prior to data collection, all children underwent an adaptation involving a child-appropriate explanation of the procedure and contact with the scanner to increase compliance and decrease motion artifacts (Raschle et al., 2012).

Raw imaging data was stored in DICOM format (Digital Imaging and Communications in Medicine). To secure consistency of the data set, information for each header file was reviewed manually to secure consistent protocol properties (Table 4 and 5). The data was retrieved with the "dicomread" tool from the python-language-based pydicom package (https://github.com/darcymason/pydicom). Only images with the following characteristics were included in the analysis:

Parameter	Value
Field of View	256 x 256mm
b-value	1000s/mm^2
Number of diffusion gradients	30 + 10 b0 images
Size (number of voxels)	128/128/64
Repetition time	8320ms
Echo time	88ms
Spacing	2mm x 2mm x 2mm

Table 4 Parameters of acquired diffusion weighted imaging (DWI) data sets.

Parameter	Value
Field of View	220 x 220mm
Size (number of voxels)	256/256/128
Repetition time	2270ms
Echo time	1450ms
Spacing	1.1mm x 1.1mm x 1.0mm

Table 5 Parameters of acquired T1 weighted data sets.

4.2.2 MRI data preprocessing

4.2.2.1 Data quality assessment

For further processing, DICOM files were transformed into Nearly Raw Raster Data (nrrd) format using the "DWIConvert" tool from the 3D Slicer software, Version 4.4.0 (Surgical Planning Laboratory, Boston, United States) (Fedorov et al., 2012). The data was then visualized for the review of quality using the aforementioned 3D Slicer software, Version 4.4.0 (Surgical Planning Laboratory, Boston, United States) (Fedorov et al., 2012). The quality of each complete data set was manually reviewed to ensure reliability of the results (Roalf et al., 2016). T1-weighted images with motion artefacts such as the ringing-phenomenon, as well as DWI with more than five diffusion gradients with motion artifacts also resulted in exclusion (Figure 4). Detailed distributions of the acquired and excluded scans can be found in Tables 6 and 7.

DWI data sets	Acquired	Motion artifacts	Varying properties	Excluded total	Included total
Baseline	50	12	7	19	31
1st follow up	53	7	6	13	40
2nd follow up	52	6	7	13	39
3rd follow up	39	8	2	10	29
4th follow up	22	2	5	7	15
5th follow up	19	2	3	5	14
6th follow up	9	1	0	1	8
Total	244	38	30	68	176

Table 6 Summary of included and excluded diffusion weighted imaging (DWI) data sets**.**
Varying properties summarizes datasets with either of different acquisition parameters such as repetition or time and incomplete data due to interruption in the acquisition.

T1 data sets	Acquired	Motion artifacts	Varying properties	Excluded total	Included total
Baseline	91	21	2	23	68
1st follow up	88	19	0	19	69
2nd follow up	59	12	0	12	37
3rd follow up	49	11	3	14	35
4th follow up	27	3	1	4	23
5th follow up	19	2	0	2	17
6th follow up	9	2	0	2	7
Total	342	70	6	76	266

Table 7 Summary of included and excluded T1 weighted images**.**
Varying properties summarizes datasets with either of different acquisition parameters such as repetition or time and incomplete data due to interruption in the acquisition.

Examples of motion artifacts considered to be low quality are illustrated in Figure 4.

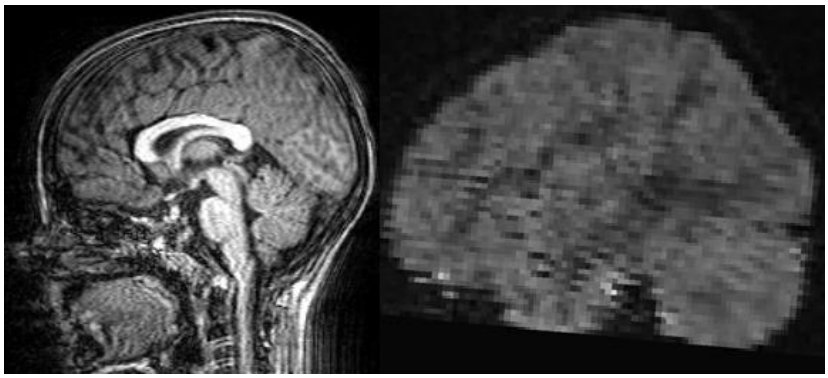

Figure 4: Examples of motion artefacts in structural (left) and diffusion imaging (right).

4.2.2.2 DWI data preprocessing

Following the exclusion of DWI datasets with insufficient quality, the 176 data sets underwent correction for the distorting eddy currents (Zhuang et al., 2006). This correction was performed with a python-language based correction script from the pipeline built at the Psychiatry and Neuroimaging Laboratory (https://github.com/pnlbwh/pnlutil/ tree/master/pipeline). The images were aligned to the axis through the anterior and posterior commissure using 3D Slicer software (Version 4.4.0) (Fedorov et al., 2012, Rohde et al., 2004, Jezzard et al., 1998). Then, DWI data masking was performed using the semi-automated masking tool from the "diffusion weighted images" module of the 3D Slicer and later manually reviewed for quality (Fedorov et al., 2012). During quality inspection, any falsely identified brain and non-brain tissue was manually corrected to be recognized as such.

Moreover, since GM is located in proximity to the highly diffusive cerebrospinal fluid compartment (CSF), partial volume effects are a potential confounding factor of the diffusion signal of the cortex (Panagiotaki et al., 2012, Pasternak et al., 2009). Therefore, prior to tensor estimation, the data sets were corrected for free-water. The correction was performed by removal of the free-water signal component from the voxel following the assumption that the diffusion coefficient in the CSF is three times higher than in the cerebral cortex (Holz, 2000, Helenius et al., 2002). A MATLAB software-based script (Natick, Massachusetts: The MathWorks Inc.) (The MathWorks, 2015) provided by Dr. Pasternak was used for this, and the resulting free-water corrected diffusion tensor maps were later used for the HG estimation.

4.2.2.3 Structural data preprocessing

The preprocessing of 266 structural T1-weighted images consisted of mask creation, segmentation and a review of the segmentation quality with optional correction and co-registration to the DWI space. The FreeSurfer software (Version 5.3) was used for masking with the "skull-strip" function (Fischl, 2012). Subsequently the FreeSurfer-based recon-all was used for cortical parcellation and subcortical segmentation yielding 183 labels from the Desikan atlas (45 subcortical GM labels, 70 WM labels and 68 cortical GM labels in both hemispheres) (Desikan et al., 2006, Fischl, 2012). The results were manually reviewed at each slice to detect incorrect segmentations. In cases where the WM-GM boundary was not identified correctly, an exact segmentation was facilitated by manually placing fiducials in WM. These fiducials are used by the software to adapt segmentation in the repeated process.

Thereafter, FreeSurfer label maps were co-registered on the DWI using an in-house non-linear registration python-based pipeline. The pipeline relies on the (Johnson, 2018). The registration tools included packages from the Advanced Normalization Tools (ANTs) software (Avants et al., 2011).

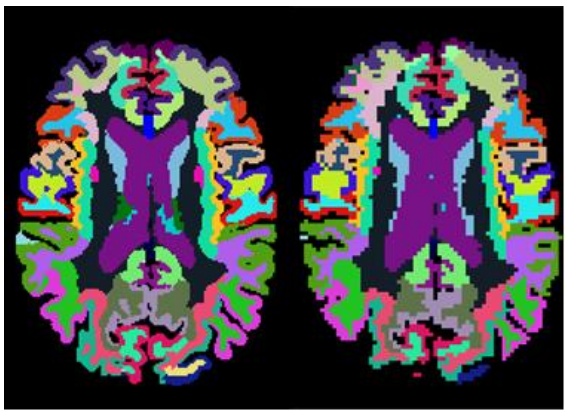

Figure 5 Cortical segmentation in native and DWI space based upon Left: FreeSurfer segmentation. Right: Segmentation after non-linear registration onto the DWI data. The lower resolution of the registered segmentations is caused by the lower resolution of the diffusion MRI image.

4.3 Obtaining HG measures

The computation of HG values was performed using the script kindly shared by Rathi et al. (Rathi et al., 2014). HG was computed from FreeSurfer label maps in the DWI space and free-water corrected DWI information using the following equation:

$$H(m) = \frac{1}{N^2}\sum_{i=1}^{N}\sum_{j=1}^{N}||m_i - m_j||$$

where m is the diffusion metric (FA or MD) indexed by i and j, and N denotes the number of voxels in the ROI. The HG for FA and MD was estimated within the unit consisting of all lobar labels listed below. The computation of variability was performed with MATLAB Software version 2015a (The MathWorks, 2015). The labels – presented below in the same way as available in the FreeSurfer aparc and wmparc files were used to merge into each lobe (Desikan et al., 2006). Single labels were merged into a larger ROI since HG is more likely to be increased, if the ROI contains areas with and without expected structure alterations. Furthermore, from algebraic point of view, HG, representing variability, calculated within a lobe is much more reliable due to the higher number of voxels.

1) Frontal lobe: caudal middle frontal, caudal anterior cingulate, paracentral, pars opercularis, pars orbitalis, pars triangularis, rostral anterior cingulate, rostral middle frontal, superior frontal, lateral orbitofrontal, medial orbitofrontal, precentral, frontal pole.
2) Temporal lobe: inferior temporal, middle temporal, fusiform, entorhinal, superior temporal, temporal pole, transverse temporal, parahipocampal.
3) Parietal lobe: inferior parietal, superiorparietal, supramarginal, precuneus, postcentral, posterior cingulate, isthmus cingulate.

The HG values were computed for GM and WM on each hemisphere thus resulting in 12 ROIs. The WM ROIs consisted of WM labels with the same names, as these are segmented in FreeSurfer based on the cortical region located above.

4.4 The Lateralization Index (LI)

To investigate potential inter-hemispherical differences, the Lateralization Index (LI) was calculated, as described in previous investigations on the WM microstructure in DD (Vandermosten et al., 2013). The term for LI computation can be expressed as:

$$LI(HG) = \frac{right\ ROI\ (HG) - left\ ROI\ (HG)}{right\ ROI\ (HG) + left\ ROI\ (HG)}\ x\ 100$$

where *HG* is the HG of the diffusion measure, and ROI is the region of interest for which the index was calculated.

4.5 Statistical analysis

Both descriptive and inferential statistics were performed with R software version 3.6.0 (R Foundation for Statistical Computing, Vienna, Austria (June 5th 2015) (R_Development_Core_Team, 2008)). For between-group comparison two-sided t-tests were performed for continuous, normally distributed data (age, KBIT and HLE) and Fisher's exact test was employed for variables at categorical scale (gender and handedness). Neurobehavioral scores were also compared with a two-sided t-test between groups, as normal distribution was assumed in the testing battery.

In contrast to IQ, home literacy was not included as a covariate in the analysis of covariance, because it is not a behavioral measure for each individual. Furthermore, from the mathematical approach, increasing the number of covariates in trials with relatively low participant numbers is critical due to the risk of overfitting as a result of the low ratio between degrees of freedom and the number of covariates.
Analysis of co-variance (ANCOVA) was introduced for hypothesis testing, with four different models.

In Analysis A, the following model was used to test for the effect of FHD status:

$$HG \sim family\ history + age + handedness + IQ + gender$$

In Analysis B, the following model was used to test for the influence of phenotype status:

$$HG \sim phenotype\ + age + handedness + IQ + gender$$

where phenotype was a categorical variable coding the reading performance status (poorly or well-performing reader).

In Analysis C, the following model was used to test for the influence of combined reading status, considered as phenotype, and FHD+ as putative genotype status:

$$HG \sim genotype\_phenotype + age + handedness + IQ + gender$$

The genotype_phenotype status was a combined categorical variable with poorly performing FHD+ individuals and normally performing FHD- controls. Poorly performing FHD- participants were not included. The aim of the analysis was to investigate symptomatic individuals at genetic risk in comparison to well-performing controls. A row of different factors contributing to low performance in FHD- may exist; however, it is not within the scope of this analysis.

In Analysis D, the following model was used to test whether HG is linked to later reading performance:

$$HG_B \sim RAN_{FU} + CTOPP_{FU} + age_B + handedness_B + IQ_B + gender_B$$

where the RAN and CTOPP values were the follow-up measures after two years of reading education. Only the age at baseline was chosen to be a covariate, as age contributes to HG (Rathi et al., 2014).

4.5.1 Significance level and correction for multiple comparisons

In all of the following analyses, the significance level was set to $p = 0.05$. In addition, the "false discovery rate" was used to correct for multiple comparisons (Streiner and Norman, 2011). As part of the statistical analysis it was performed using the fdr-tool from the R package (Version 6.3.0) (R_Development_Core_Team, 2008).

5 **Results**

5.1 HG assessment in FHD+ children and poor readers

5.1.1 Analysis A: HG in children with family history of DD

The analysis of the HG of FA and MD in the frontal, temporal, and parietal GM as well as in WM did not reveal any significant relation to FHD status. There were no tendencies of HG's lateralization index between groups.

Prior to the correction for multiple comparisons, the left hemispheric frontal WM HG of MD was higher in individuals with FHD+ ($p=0.057$ after and $p=0.009$ prior to correction for multiple comparisons, also see Figure 7). Of note, age had an effect on HG of MD in the right frontal and left parietal cortex (Figure 6). This effect did not remain significant after correction for multiple comparisons. Importantly, age was included as a covariate in all analyses. There was no difference in RAN ($p=0.44$) or CTOPP ($p=0.89$) between groups.

Results of Analysis A are reported in detail in Tables 12-15 in section 7.1. The demographic data is illustrated below, in Table 8.

Item	FHD-	FHD+	p-value
N(participants)	30	25	-
Gender ratio (♀:♂)	15:15 (50.00%:50.00%)	11:14(44.00%:56.00%)	0.788^{A}
Mean age in months (σ)	96.01 (19.43)	102.05 (21.55)	0.293^{B}
Age range in months	67.74 – 137.26	73.52 – 150.43	-
Handedness (left:right)	2:28	4:21	0.394^{A}
Non-verbal IQ (σ)	102.37 (10.13)	102.68 (13.16)	0.924^{B}
Home literacy (σ)	32686.42 (9109.88)	28747. (11595.94)	0.228^{B}

Table 8 Demographic data in Analysis A. Groups based on family history for developmental dyslexia (DD), A: Fisher's exact test; B: t-test.

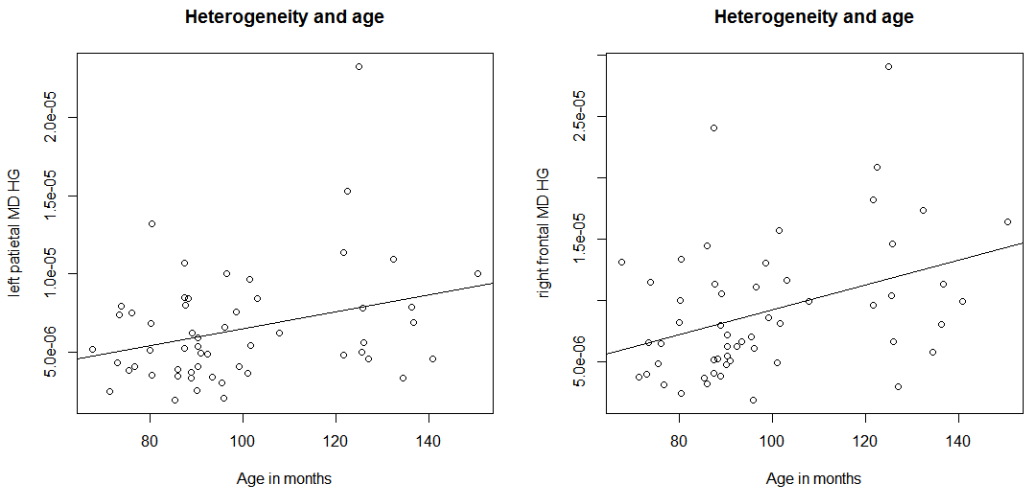

Figure 6 Scatterplots of mean diffusivity (MD) heterogeneity (HG) in left parietal (left) and right frontal cortex (right) that showed a tendency of correlating with age (both p=0.284).

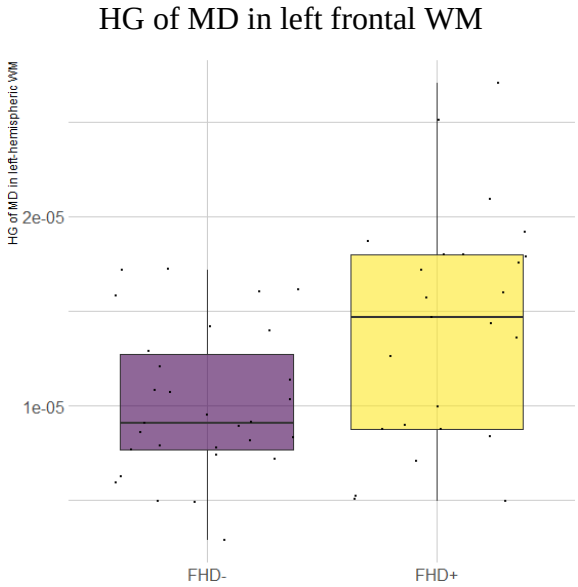

Figure 7 Boxplot depicting left frontal WM heterogeneity differences in children risk for dyslexia. Tendency of higher mean diffusivity (MD) heterogeneity (HG) in left frontal WM in children with positive family history of dyslexia (p=0.057 after correction for multiple comparisons).

5.1.2 Analysis B: HG in poor readers

9 out of 15 participants in the group of poor readers were FHD+ children. 14 of 27 individuals in the control group had FHD+ status. The comparison of demographic factors did not reveal statistical differences between the group of poorly performing readers and well-reading controls regarding age, gender distribution, handedness, or home literacy environment. However, a significantly lower mean non-verbal IQ was measured in the group of impaired readers (p=0.0007). Summary of the demographic

information is depicted below, in Table 9. There were also no statistically significant findings for HG in GM or WM, and no differences between groups in the lateralization index. The results for analysis B are summarized in Tables 16-19 in section 7.2.

Item	Normal readers	Impaired readers	p-value
N(participants)	27	15	-
Gender ratio (♀:♂)	14:13 (51.85%:48.15%)	9:6 (60%:40%)	0.750 [A]
Mean age in months (σ)	92.49 (19.76)	102.67 (24.92)	0.2451 [B]
Age range in months	71.39 – 136.24	67.74 – 150.43	-
Handedness (left:right)	3:24	3:12	0.649 [A]
Non-verbal IQ (σ)	105.19 (9.90)	95.00 (7.29)	0.0007 [B]
Home literacy (σ)	33041.00 (11481.37)	27413.73 (7222.29)	0.1194 [B]

Table 9 Demographic data in Analysis B. Groups based on reading performance, A: Fisher's exact test; B: t-test.

5.1.3 Analysis C: HG in poor FHD+ readers

The HG of FA and MD in GM and WM, as well as the corresponding LI, did not differ between FHD+ children with impaired reading skills and controls after correction for multiple comparisons. Detailed outcomes are presented in Tables 20-23 in section 7.3. Similar to Analysis A, there was higher HG of MD in the left frontal WM, but it did not remain significant after correction for multiple comparisons (p=0.35, p=0.032 prior to the correction). Figure 8 illustrates the trend toward a higher HG in individuals at risk. Furthermore, there were no differences between groups in age, gender distribution, and handedness, while poor FHD+ readers had lower home literacy and non-verbal IQ than controls (respectively p=0.029 and p=0.010), as illustrated in Table 10.

Item	FHD-	FHD+	p-value
N(participants)	14	5	
Gender ratio (♀:♂)	8:6 (57.14%:42.86%)	2:3 (40.00%:60.00%)	0.629[A]
Mean age in months (σ)	95.31 (21.59)	121.68 (26.00)	0.117
Age range in months	71.39 – 137.26	90.21 – 150.43	-
Handedness (left:right)	2:12	3:2	0.084[A]
Non-verbal IQ (σ)	106.7 (9.89)	92.8 (6.82)	0.010[B]
Home literacy (σ)	33167.7 (11777.20)	21099.6 (5905.46)	0.029[B]

Table 10 Demographic data in Analysis C. Groups based on combined positive family history of dyslexia (FHD+) status and reading performance. A: Fisher's exact test; B: t-test

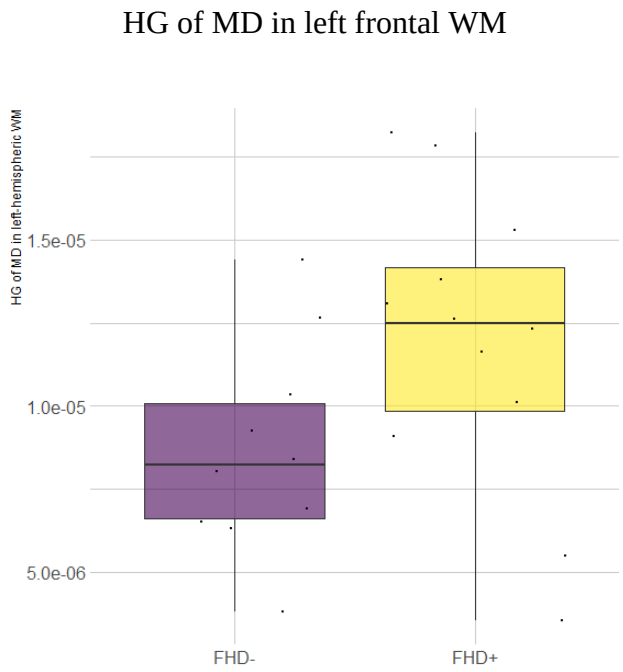

Figure 8 Boxplot depicting left frontal WM heterogeneity differences in children risk for dyslexia with worse reading performance. Tendency of higher mean diffusivity (MD) heterogeneity (HG) in left frontal white matter (WM) in children with positive family history of dyslexia and low reading performance (p=0.35 after correction for multiple comparisons).

5.2 Testing for the second hypothesis: HG in diffusion as a prognostic measure of reading performance

5.2.1 Analysis D: HG as a predictor for reading performance

The HG of FA and MD in GM and WM, as well as the corresponding LI did not predict the RAN or CTOPP values after correction for multiple comparisons. Prior to this correction, the HG of MD in left parietal GM was positively associated with later rapid naming performance RAN (p=0.043 prior to correction for multiple comparisons), as depicted in Table 24 in section 7.4. Figure 9 illustrates the tendency of relationship of HG as the function of RAN at follow up.

There were in total 22 participants with a higher female to male ratio. There were 3 left-handed individuals. The sample's demographic characteristics are presented in Table 11.

Item	Number of participants
N(participants)	22
Gender ratio (♀:♂)	16:6
Mean age in months(σ)	65.86 (5.21) months
Age range in months	59.30 – 79.27 months
Handedness (left:right)	3: 19
Non-verbal IQ (σ)	99.98 (11.32)

Table 11 Demographic data in Analysis D. Group tested for heterogeneity (HG) as predictor for rapid naming and phonologic processing

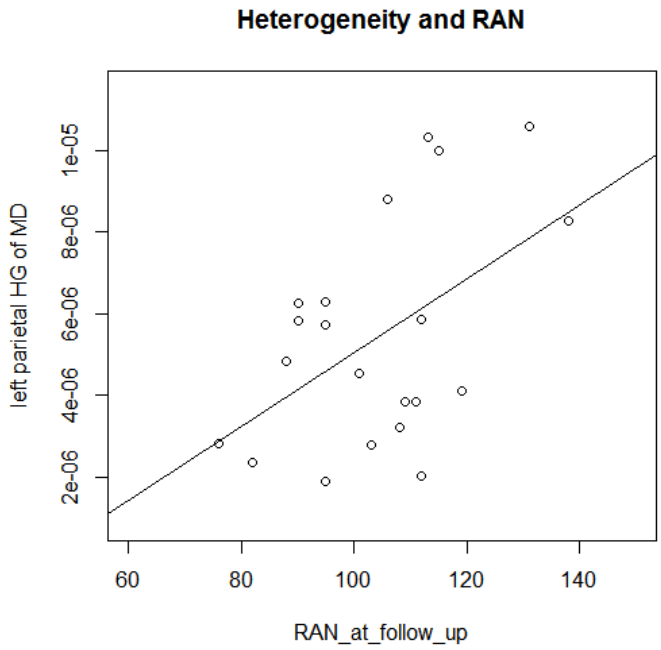

Figure 9 Correlational relationship in a linear model between heterogeneity (HG) of mean diffusivity (MD) in left parietal cortex and rapid naming (RAN).

6 Discussion

The aim of this study was to use the HG of diffusion metrics to investigate the microstructure of GM and WM in the frontal, parietal and temporal lobes of children at increased genetic risk for DD. Two hypotheses were tested: First, FHD+ individuals exhibit increased HG of diffusion due to mutations causing altered GM and WM microstructure. Second, HG at pre-school age (before learning to read) predicts future rapid naming and phonologic processing skills.

Testing of the first hypothesis was done in three analyses. Analysis A revealed no significant differences between FHD+ children and controls. There was a tendency for higher MD HG in the frontal WM of FHD+ children. A similar tendency was observed in the sub-group consisting of children with both FHD+ and poor reading skills (Analysis C). Analysis B showed no differences in WM and GM HG between well and poorly performing readers, independent of genetic risk status. The analysis for the second hypothesis also did not yield any statistically significant findings, only a tendency of MD HG in the left parietal cortex being positively associated with future rapid naming skills.

6.1 HG in individuals at risk for DD and in impaired readers

6.1.1 Conclusions from the analysis of individuals at risk for DD

Since differences in the HG of frontal WM were not observed after correction for multiple comparisons (Analysis A), the first hypothesis cannot be verified based on the cohort tested. Nevertheless, the data indicates a tendency of a higher HG of MD in children at risk for DD. This is in line with the previously observed location of altered diffusion measures in left hemispheric frontal WM in impaired readers (Rimrodt et al., 2010, Odegard et al., 2009, Partanen et al., 2020). MD is usually high in regions with fewer structures obstructing diffusion, such as GM or cerebrospinal fluid, whereas it is lower in WM due to the tightly organized axons with lipid-rich myelin hindering diffusion perpendicular to the main axis (Selemon and Goldman-Rakic, 1999, Mori, 2007). Higher HG of MD in the frontal lobes of children with FHD+ represents an increased variability of MD values within the region of interest (frontal lobe). This finding may suggest altered neuronal migration potentially leading to heterotopic GM

scattered throughout the WM of the frontal lobe. Small groups of heterotopic neural GM tissue are an intuitive explanation for such scattered increase in MD in WM.

Lack of statistically significant finding may rely on lack of statistical power. In particular, in larger cohorts, a stronger effect might be observable in FHD+ children, who have not yet received reading training. Such an approach would account for potential compensatory mechanisms.

It can further be assumed that the differences in HG between groups would be stronger if the participants were assigned to groups based on actual diagnosed genetic mutations instead of genetic risk. In such a case, all participants in a subgroup would be mutation carriers. In contrast, despite lack of information on prevalence an inheritance of specific mutations current literature indicates that FHD+ individuals have a 50% chance to develop DD (Hallgren, 1950, Grigorenko, 2001, Chang et al., 2005, Raschle et al., 2011, Adler et al., 2013).

Another reason for the lack of statistical significance between groups could be due to lack of sensitivity of the method. The alterations of GM found in DD include microscopic alterations in the six-layered neocortex (Galaburda and Kemper, 1979). In light of the available DWI resolution with a voxel size of 2 x 2 x 2mm, the insufficient, almost macroscopic, resolution might have missed subtle microscopic aberrations. A higher resolution contributing to a higher number of smaller voxels would detect small variations more sensitively. The lack of sensitivity also concerns the possibility that the lobar ROIs are too large for HG to detect a difference, for example, in a cerebral gyrus.

Despite earlier reports on leftward lateralization of microstructural WM abnormalities in impaired readers, the lateralization index did not display any significant relationships with HG (Im et al., 2013, Banfi et al., 2019, Vandermosten et al., 2013, Yeatman et al., 2011). Concluding from similar lateralization degree, the results do not support the existing assumption on leftward pathology or rightward compensation processes in children at risk for DD (Vandermosten et al., 2013).

6.1.2 Conclusions from the analysis on poor readers

Analysis B did not reveal any statistically significant differences in the HG of GM and WM between those with poor reading performance compared to those with good reading performance and independent of their genetic risk status. In contrast to Analyses A and C, no tendencies could be observed, suggesting that there is no association between HG and reading phenotype. Even though it is an intuitive observation, that the group without specific risk for genetic mutations linked with DD did not display the tendencies observed in the WM of other groups, it stands in contrast to existing literature. As presented in the review on DWI findings in poor readers (see Table 3, section 3.3) there are several studies linking left-hemispheric WM DWI findings to reading function in poor readers (Steinbrink et al., 2008, Gebauer et al., 2012, Partanen et al., 2020, Su et al., 2018). Of note the group of poor readers in this study displayed lower non-verbal IQ potentially confounding the results.

6.1.3 Conclusions from the analysis on poor readers at risk

The tendency of increased MD HG in left frontal WM from Analysis A was also observed in a sub-group of FHD+ children with lower reading measures, as illustrated in Figure 7 in chapter 5.1.3. Nevertheless, the low number of participants should be kept in mind when discussing this finding. Moreover, the extent to which the differences would gain in effect if smaller ROIs were chosen, is unclear. A Focus on smaller areas could potentially contribute to higher HG. For example, microstructural abnormality in a sub-part of one of the temporal gyri would contribute more strongly to higher HG if it was calculated separately for each gyrus. From an arithmetic point of view, such an approach would, however, artificially sharpen the results, as variability can easily be increased with a smaller sample size of included voxels. Since the genetic mutations described in the introduction are thought to contribute to altered neuronal migration in wide parts of the brain it is assumed that differences would also be detectable in a larger ROI.

6.1.4 Conclusion on heterogeneity and genetic risk for DD

HG was not statistically significantly different in the two groups or the subgroup compared to controls. Therefore, the hypothesis of increased HG in FHD+ participants cannot be verified and must thus be rejected based on the sample analyzed here. The

small size of the cohorts might have led to the lack of statistically significant differences. Considering the observed tendencies, studies in larger cohorts and thus higher statistical power may reveal statistically significant relationships of HG with genetic risk and reading performance.

Furthermore, normal HG does not equate to a normal microstructure. The microstructure may still be altered uniformly across the brain. In such case the HG in diffusion measures in individuals with DD will remain unchanged. This is in line with previous studies that have presented altered diffusion measures in WM in DD.

6.2 HG as a predictor for future reading skills

HG did not significantly predict the later RAN and CTOPP measures. There was a tendency of increased HG in the left parietal cortex associated with increased RAN values (Table 24). The observation is surprising due to its direction, as a more heterogeneous cortical microstructure is related to faster performance. The other aspect is the localization where it occurred, since rapid naming is thought to rely on the retrieval of information from the VWFA in the fusiform gyrus (Finn et al., 2014). It was phonologic processing that was hypothesized to be linked to processing in the parietal lobe according to the two-stream hypothesis mentioned in the introduction (Boets et al., 2013, Yeatman et al., 2011). Instead of supporting it, the current results rather oppose the “dorsal and ventral stream” hypothesis (Sigurdardottir et al., 2015). The nature of this finding remains unintuitive, yet interesting. In this tendency, rapid naming seems to be facilitated by the parietal and not the temporal lobe.

The MD HG in the parietal cortex at the pre-school time point showed a tendency to predict later rapid naming performance. However, it was not different between well and poorly reading children (Analysis B). The decrease in parietal GM HG may therefore be linked to reading training at school. The latter has already been associated with changes in the mean values of FA in WM (Saygin et al., 2013). The change in HG properties to the degree of losing the trend after reading training may be an indication of neuroplasticity response in GM. This could be part of compensatory processes including pruning or synaptogenesis. The fact that despite normalization of the structure, performance is still impaired indicates that this potential compensation mechanism might not be sufficient.

6.3 Limitations

This study had some limitations that must be considered. Despite accommodation sessions with the scanner prior to the imaging sessions, a high percentage of imaging data sets had motion artefacts, which led to exclusion of data from the analyses (e.g. 68 out of 244 DWI data sets). MR imaging in children remains challenging due to susceptibility to motion and the relatively long duration of an MRI scan. Since the technique will not become more precise within a shorter time, a conservative quality assessment of data is necessary to assure result reliability.

The demographic assessment in the cross-sectional analyses in groups based on reading performance revealed different non-verbal IQs, which may have induced a bias. Individuals performing worse in RAN and CTOPP had lower IQ scores, with a mean of 95 compared to 105 in controls ($p=0.0007$). A similar discrepancy was observed in the subgroup compromising FHD+ individuals with poor reading performance ($p=0.01$). In contrast, no differences in non-verbal IQ were observed in a group purely based on risk for DD ($p=0.44$), and no correlation was found between RAN and KBIT in the prospective analysis ($p=0.77$).

The methodologic limitation is linked to HG as an innovative and exploratory technique. There are currently only two studies available and limited to findings regarding adult aging and schizophrenia (Seitz et al., 2018, Rathi et al., 2014). Additional studies in different cohorts are required to understand the HG observations to a higher extent. The need for such validation is necessary, especially because this work was the first to assess HG in WM, as the work in both available articles focused on GM HG.

6.4 Future perspectives

The results of this work show tendencies of altered WM structure in children at risk for DD and a trend of correlation between microstructure and later reading skills. These tendencies shed light on potential relationships between microstructure and function. This work introduced a novel measure of brain tissue microstructure that may be related to developmental microstructural alterations. Future studies on cortical and subcortical microstructure are needed to investigate the association between different diffusion

measures. Furthermore, studies should include larger samples to increase statistical power.

Regarding the methodology, an interesting consideration would be to use HG in more specific ROIs, such as the superior temporal gyrus. Its macrostructure has previously been linked to reading impairment (Richlan et al., 2013). If a potential abnormality in microstructure is localized, then its statistical influence will be weakened if using a larger ROI. In such a case, examining an even higher number of participants would be crucial, since HG as a measure of variability relies on variance. In turn, statistical testing of variance in an ROI with a smaller number of voxels would require higher sample sizes to sustain the statistical power.

6.5 Conclusion

HG of GM and WM was not significantly different between controls and FHD+ individuals or individuals with poor reading skills. It was also not different in the sub-group of FHD+ individuals with poor reading skills. HG also did not significantly predict rapid naming and phonologic skills.

Nonetheless, the analyses revealed a tendency of increased MD HG in left frontal WM in FHD+ individuals. This observation might be potentially related to GM heterotopia within the WM. Analyses on larger cohorts may yield significant results in the future. The second observation included a trend of parietal HG of GM at pre-school age predicting later rapid naming abilities. This finding was surprising, since rapid naming was rather expected to be linked to the structure of inferior temporal areas. The absence of differences in parietal HG between good and poor readers after receiving reading training could suggest compensation with neuroplastic processes such as synaptogenesis or pruning. However, these observations should be investigated in detail in larger cohorts.

Taken together, the tendencies point toward the assumed link between genetic mutations associated with DD and brain tissue microstructure.

7. Supplementary material

7.1 Analysis A – HG and genetic risk for DD

ROI	FHD	Age	HND	IQ	gender	p (F statistic)	R^2
HFA left frontal	0.467	0.162	0.098	0.870	0.685	0.442	0.017
HFA right frontal	0.232	0.103	0.280	0.705	0.562	0.442	0.023
HFA left parietal	0.579	0.216	0.266	0.951	0.304	0.442	0.007
HFA right parietal	0.500	0.093	0.528	0.921	0.498	0.442	0.004
HFA left temporal	0.957	0.077	0.160	0.569	0.810	0.284	0.018
HFA right temporal	0.991	0.095	0.252	0.415	0.660	0.442	0.02
HMD left frontal	0.641	0.075	0.156	0.687	0.127	0.442	0.101
HMD right frontal	0.307	0.007	0.324	0.879	0.453	0.284	0.118
HMD left parietal	0.410	0.053	0.311	0.159	0.257	0.284	0.129
HMD right parietal	0.583	0.031	0.386	0.365	0.457	0.421	0.079
HMD left temporal	0.224	0.193	0.877	0.640	0.391	0.442	0.005
HMD right temporal	0.425	0.183	0.691	0.580	0.588	0.561	0.019

Table 12 Heterogenetiy (HG) in gray matter (GM) of individuals at higher genetic risk for dyslexia FHD: family history status, HND: Handedness, KBIT: non-verbal IQ, HFA and HMD: HG of FA and MD. The values represent significance level of variables' influence on HG. The last p-value corresponds to the F-statistic and is corrected for multiple comparisons. R^2describes the models multiplied R^2.

ROI	FHD	Age	HND	KBIT	gender	p (F statistic)	R^2
HFA left frontal	0.307	0.106	0.666	0.993	0.738	0.686	0.088
HFA right frontal	0.0374	0.095	0.530	0.640	0.246	0.209	0.183
HFA left parietal	0.631	0.290	0.973	0.849	0.287	0.727	0.069
HFA right parietal	0.697	0.925	0.745	0.808	0.900	0.995	0.134
HFA left temporal	0.9359	0.488	0.743	0.086	0.722	0.686	0.081
HFA right temporal	0.639	0.856	0.658	0.072	0.200	0.528	0.112
HMD left frontal	0.005	0.099	0.117	0.285	0.307	0.057	0.260
HMD right frontal	0.487	0.537	0.548	0.485	0.731	0.905	0.042
HMD left parietal	0.076	0.482	0.608	0.002	0.343	0.057	0.267
HMD right parietal	0.321	0.347	0.787	0.049	0.276	0.444	0.138
HMD left temporal	0.061	0.149	0.501	0.093	0.115	0.165	0.205
HMD right temporal	0.262	0.149	0.874	0.154	0.919	0.465	0.167

Table 13 Heterogenetiy (HG) in white matter (WM) of individuals at higher genetic risk for dyslexia FHD: family history status, HND: Handedness, KBIT: non-verbal IQ, HFA and HMD: HG of FA and MD. The values represent significance level of variables' influence on HG. The last p-value corresponds to the F-statistic and is corrected for multiple comparisons. R^2 describes the models multiplied R^2.

ROI	FHD	Age	HND	KBIT	gender	p (F statistic)	R^2
HFA LI frontal	0.159	0.441	0.107	0.519	0.595	0.839	0.127
HFA LI parietal	0.736	0.400	0.213	0.702	0.374	0.971	0.070
HFA LI temporal	0.883	0.885	0.756	0.666	0.283	0.971	0.031
HMD LI frontal	0.570	0.264	0.177	0.708	0.080	0.839	0.117
HMD LI parietal	0.693	0.804	0.662	0.597	0.666	0.971	0.024
HMD LI temporal	0.386	0.796	0.867	0.942	0.896	0.831	0.017

Table 14 Heterogeneity (HG) lateralization index (LI) in gray matter (GM) of individuals at higher genetic risk for dyslexia
FHD: family history status, HND: Handedness, KBIT: non-verbal IQ, HFA and HMD HG of FA and MD. The values represent significance level of variables' influence on HG. The last p-value corresponds to the F-statistic and is corrected for multiple comparisons. R^2describes the models multiplied R^2.

ROI	FHD	Age	HND	KBIT	gender	p (F statistic)	R^2
HFA LI frontal	0.137	0.973	0.783	0.529	0.239	0.971	0.086
HFA LI parietal	0.944	0.079	0.573	0.952	0.157	0.939	0.141
HFA LI temporal	0.502	0.499	0.924	0.870	0.240	0.971	0.045
HMD LI frontal	0.008	0.187	0.093	0.778	0.278	0.380	0.215
HMD LI parietal	0.751	0.839	0.970	0.533	0.314	0.971	0.032
HMD LI temporal	0.907	0.645	0.744	0.829	0.306	0.971	0.041

Table 15 Heterogeneity (HG) lateralization index (LI) in white matter (WM) of individuals at higher genetic risk for dyslexia
FHD: family history status, HND: Handedness, KBIT: non-verbal IQ, HFA and HMD: HG of FA and MD. The values represent significance level of variables' influence on HG. The last p-value corresponds to the F-statistic and is corrected for multiple comparisons. R^2describes the models multiplied R^2.

7.2 Analysis B – HG and reading performance

ROI	IR	Age	HND	KBIT	gender	p(F statistic)	R^2
HFA left frontal	0.869	0.938	0.656	0.928	0.348	0.969	0.039
HFA right frontal	0.648	0.743	0.410	0.943	0.350	0.969	0.067
HFA left parietal	0.507	0.986	0.518	0.769	0.155	0 969	0.094
HFA right parietal	0.682	0.948	0.263	0.768	0.359	0.969	0.076
HFA left temporal	0.487	0.689	0.666	0.791	0.743	0.969	0.031
HFA right temporal	0.785	0.716	0.976	0.999	0.394	0.969	0.034
HMD left frontal	0.909	0.449	0.200	0.861	0.702	0.969	0.070
HMD right frontal	0.972	0.372	0.458	0.974	0.846	0.969	0.038
HMD left parietal	0.359	0.375	0.868	0.952	0.802	0.969	0.059
HMD right parietal	0.641	0.535	0.771	0.874	0.941	0.969	0.024
HMD left temporal	0.863	0.391	0.528	0.629	0.767	0.969	0.058
HMD right temporal	0.008	0.831	0.945	0.131	0.419	0.969	0.211

Table 16 Heterogenetiy (HG) in gray matter (GM) of impaired readers
IR: impaired readers, HND: Handedness, KBIT: non-verbal IQ, HFA and HMD: HG of FA and MD. The values represent significance level of variables' influence on HG. The last p-value corresponds to the F-statistic and is corrected for multiple comparisons. R^2 describes the models multiplied R^2.

ROI	IR	Age	HND	KBIT	gender	p(F statistic)	R^2
HFA left frontal	0.441	0.829	0.097	0.995	0.250	0.786	0.142
HFA right frontal	0.596	0.730	0.149	0.718	0.190	0.786	0.141
HFA left parietal	0.766	0.829	0.534	0.504	0.091	0.786	0.128
HFA right parietal	0.580	0.506	0.477	0.516	0.218	0.918	0.083
HFA left temporal	0.123	0.974	0.373	0.729	0.197	0.786	0.169
HFA right temporal	0.155	0.975	0.778	0.289	0.171	0.721	0.208
HMD left frontal	0.355	0.198	0.399	0.568	0.997	0.786	0.113
HMD right frontal	0.293	0.633	0.876	0.315	0.795	0.918	0.044
HMD left parietal	0.680	0.605	0.344	0.549	0.554	0.918	0.038
HMD right parietal	0.170	0.735	0.859	0.131	0.472	0.786	0.106
HMD left temporal	0.209	0.846	0.377	0.895	0.872	0.721	0.075
HMD right temporal	0.682	0.609	0.601	0.563	0.458	0.918	0.060

Table 17 Heterogenetiy (HG) in white matter (WM) of impaired readers
IR: impaired readers, HND: Handedness, KBIT: non-verbal IQ, HFA and HMD: HG of FA and MD. The values represent significance level of variables' influence on HG. The last p-value corresponds to the F-statistic and is corrected for multiple comparisons. R^2 describes the models multiplied R^2.

ROI	IR	Age	HND	KBIT	gender	p(F statistic)	R^2
HFA LI frontal	0.391	0.510	0.171	0.663	0.982	0.915	0.089
HFA LI Parietal	0.420	0.844	0.136	0.988	0.104	0.915	0.167
HFA LI Temporal	0.423	0.830	0.465	0.610	0.326	0.915	0.059
HMD LI Frontal	0.940	0.428	0.300	0.766	0.300	0.915	0.081
HMD LI Parietal	0.280	0.805	0.973	0.671	0.750	0.915	0.040
HMD LI Temporal	0.005	0.257	0.977	0.017	0.223	0.844	0.238

Table 18 Heterogeneity (HG) lateralization index (LI) in gray matter (GM) of impaired readers
IR: impaired readers, HND: Handedness, KBIT: non-verbal IQ, HFA and HMD: HG of FA and MD. The values represent significance level of variables' influence on HG. The last p-value corresponds to the F-statistic and is corrected for multiple comparisons. R^2 describes the models multiplied R^2.

ROI	IR	Age	HND	KBIT	gender	p(F statistic)	R^2
HFA LI Frontal	0.640	0.892	0.696	0.504	0.742	0.914	0.038
HFA LI Parietal	0.571	0.099	0.851	0.996	0.402	0.914	0.157
HFA LI Temporal	0.838	0.896	0.507	0.387	0.864	0.914	0.049
HMD LI Frontal	0.991	0.070	0.253	0.489	0.729	0.914	0.124
HMD LI Parietal	0.563	0.740	0.491	0.456	0.225	0.914	0.098
HMD LI Temporal	0.255	0.856	0.574	0.260	0.260	0.914	0.088

Table 19 Heterogeneity (HG) lateralization index (LI) in white matter (WM) of impaired readers
IR: impaired readers, HND: Handedness, KBIT: non-verbal IQ, HFA and HMD: HG of FA and MD. The values represent significance level of variables' influence on HG. The last p-value corresponds to the F-statistic and is corrected for multiple comparisons. R^2 describes the models multiplied R^2.

7.3 Analysis C – HG and poor FHD+ readers

ROI	IRR	Age	HND	KBIT	gender	p(F statistic)	R^2
HFA left frontal	0.360	0.247	0.299	0.439	0.549	0.699	0.259
HFA right frontal	0.251	0.197	0.560	0.374	0.683	0.699	0.218
HFA left parietal	0.193	0.138	0.399	0.233	0.435	0.699	0.317
HFA right parietal	0.367	0.132	0.683	0.395	0.716	0.699	0.235
HFA left temporal	0.205	0.339	0.826	0.448	0.260	0.699	0.258
HFA right temporal	0.740	0.615	0.636	0.699	0.224	0.706	0.209
HMD left frontal	0.370	0.127	0.358	0.531	0.306	0.699	0.378
HMD right frontal	0.537	0.045	0.530	0.846	0.821	0.699	0.383
HMD left parietal	0.290	0.086	0.594	0.802	0.745	0.699	0.325
HMD right parietal	0.472	0.184	0.473	0.661	0.630	0.699	0.248
HMD left temporal	0.723	0.292	0.970	0.858	0.547	0.699	0.186
HMD right temporal	0.356	0.857	0.463	0.176	0.132	0.699	0.426

Table 20 Heterogenetiy (HG) in gray matter (GM) of impaired readers at genetic risk for dyslexia

IRR: impaired readers at risk, HND: Handedness, KBIT: non-verbal IQ, HFA and HMD: HG of FA and MD. The values represent significance level of variables' influence on HG. The last p-value corresponds to the F-statistic and is corrected for multiple comparisons. R^2 describes the model's multiplied R^2.

ROI	IRR	Age	HND	KBIT	gender	p(F statistic)	R^2
HFA left frontal	0.256	0.410	0.921	0.319	0.195	0.632	0.251
HFA right frontal	0.058	0.135	0.698	0.232	0.2475	0.531	0.362
HFA left parietal	0.263	0.572	0.580	0.117	0.0807	0.531	0.340
HFA right parietal	0.432	0.940	0.990	0.509	0.287	0.864	0.123
HFA left temporal	0.247	0.641	0.959	0.548	0.116	0.594	0.282
HFA right temporal	0.415	0.786	0.967	0.971	0.40047	0.862	0.1537
HMD left frontal	0.019	0.346	0.121	0.224	0.9682	0.395	0.571
HMD right frontal	0.032	0.669	0.256	0.047	0.4671	0.531	0.479
HMD left parietal	0.213	0.376	0.190	0.255	0.415	0.531	0.356
HMD right parietal	0.359	0.242	0.479	0.230	0.185	0.531	0.319
HMD left temporal	0.674	0.059	0.087	0.583	0.3924	0.531	0.377
HMD right temporal	0.869	0.332	0.891	0.573	0.341	0.531	0.3206

Table 21 Heterogenetiy (HG) in white matter (WM) of impaired readers at genetic risk for dyslexia

IRR: impaired readers at risk, HND: Handedness, KBIT: non-verbal IQ, HFA and HMD: HG of FA and MD. The values represent significance level of variables' influence on HG. The last p-value corresponds to the F-statistic and is corrected for multiple comparisons. R^2 describes the model's multiplied R^2.

ROI	IRR	Age	HND	KBIT	gender	p(F statistic)	R^2
HFA LI Frontal	0.153	0.2698	0.084	0.435	0.478	0.729	0.354
HFA LI Parietal	0.238	0.913	0.215	0.331	0.240	0.870	0.328
HFA LI Temporal	0.025	0.252	0.364	0.417	0.402	0.729	0.384
HMD LI Frontal	0.543	0.345	0.776	0.691	0.098	0.958	0.259
HMD LI Parietal	0.503	0.793	0.607	0.897	0.747	0.958	0.070
HMD LI Temporal	0.058	0.108	0.2915	0.032	0.092	0.613	0.485

Table 22 Heterogeneity (HG) lateralization index (LI) in gray matter (GM) of impaired readers at genetic risk for dyslexia
IRR: impaired readers at risk, HND: Handedness, KBIT: non-verbal IQ, HFA and HMD: HG of FA and MD. The values represent significance level of variables' influence on HG. The last p-value corresponds to the F-statistic and is corrected for multiple comparisons. R^2 describes the model's multiplied R^2.

ROI	IRR	Age	HND	KBIT	gender	p(F statistic)	R^2
HFA LI Frontal	0.165	0.253	0.429	0.720	0.836	0.952	0.183
HFA LI Parietal	0.539	0.164	0.219	0.053	0.135	0.952	0.4721
HFA LI Temporal	0.920	0.857	0.890	0.373	0.485	0.614	0.119
HMD LI Frontal	0.871	0.330	0.771	0.454	0.567	0.958	0.194
HMD LI Parietal	0.974	0.553	0.831	0.696	0.273	0.958	0.1013
HMD LI Temporal	0.549	0.689	0.336	0.280	0.126	0.729	0.315

Table 23 Heterogeneity (HG) lateralization index (LI) in white matter (WM) of impaired readers at genetic risk for dyslexia
IRR: impaired readers at risk, HND: Handedness, KBIT: non-verbal IQ, HFA and HMD: HG of FA and MD. The values represent significance level of variables' influence on HG. The last p-value corresponds to the F-statistic and is corrected for multiple comparisons. R^2 describes the model's multiplied R^2.

7.4 Analysis D – HG as predictor for performance

ROI	RAN	CTOPP	Age	HND	KBIT	gender	p(F statistic)	R^2
HFA left frontal	0.701	0.621	0.545	0.367	0.857	0.382	0.820	0.239
HFA right frontal	0.897	0.711	0.578	0.281	0.599	0.939	0.820	0.22
HFA left parietal	0.053	0.198	0.755	0.534	0.597	0.637	0.820	0.283
HFA right parietal	0.256	0.490	0.815	0.810	0.878	0.504	0.516	0.223
HFA left temporal	0.289	0.580	0.464	0.618	0.890	0.781	0.820	0.253
HFA right temporal	0.901	0.594	0.681	0.440	0.744	0.939	0.929	0.1005
HMD left frontal	0.860	0.833	0.368	0.394	0.423	0.454	0.820	0.243
HMD right frontal	0.432	0.451	0.552	0.758	0.338	0.452	0.820	0.246
HMD left parietal	0.019	0.097	0.330	0.802	0.029	0.798	0.696	0.560
HMD right parietal	0.021	0.115	0.968	0.823	0.155	0.403	0.696	0.476
HMD left temporal	0.911	0.297	0.583	0.900	0.801	0.681	0.946	0.153
HMD right temporal	0.148	0.736	0.695	0.440	0.346	0.926	0.820	0.3006

Table 3 Heterogenetiy (HG) in gray matter (GM) as predictor for later rapid naming and phonologic performance
RAN: RAN at follow up, CTOPP: CTOPP at follow up, HND: Handedness, KBIT: non-verbal IQ, HFA and HMD: HG of FA and MD. The values represent significance level of variables' influence on HG. The last p-value corresponds to the F-statistic and is corrected for multiple comparisons. R^2 describes the model's multiplied R^2.

ROI	RAN	CTOPP	Age	HND	KBIT	gender	p(F statistic)	R^2
HFA left frontal	0.916	0.775	0.771	0.445	0.771	0.469	0.894	0.1661
HFA right frontal	0.891	0.430	0.545	0.227	0.085	0.427	0.727	0.247
HFA left parietal	0.945	0.252	0.998	0.445	0.846	0.347	0.727	0.1945
HFA right parietal	0.485	0.348	0.293	0.548	0.427	0.319	0.727	0.298
HFA left temporal	0.717	0.703	0.597	0.878	0.262	0.793	0.727	0.261
HFA right temporal	0.680	0.461	0.725	0.401	0.436	0.854	0.727	0.246
HMD left frontal	0.602	0.524	0.820	0.367	0.658	0.478	0.727	0.225
HMD right frontal	0.956	0.930	0.525	0.565	0.089	0.804	0.678	0.450
HMD left parietal	0.878	0.841	0.214	0.717	0.093	0.823	0.678	0.449
HMD right parietal	0.946	0.643	0.542	0.719	0.194	0.820	0.726	0.361
HMD left temporal	0.266	0.612	0.044	0.966	0.101	0.047	0.678	0.492
HMD right temporal	0.923	0.353	0.353	0.193	0.883	0.320	0.678	0.325

Table 25 Heterogenetiy (HG) in white matter (WM) as predictor for rapid naming and phonologic performance
RAN: RAN at follow up, CTOPP: CTOPP at follow up, HND: Handedness, KBIT: non-verbal IQ, HFA and HMD: HG of FA and MD. The values represent significance level of variables' influence on HG. The last p-value corresponds to the F-statistic and is corrected for multiple comparisons. R^2 describes the models multiplied R^2.

ROI	RAN	CTOPP	Age	HND	KBIT	gender	p(F statistic)	R^2
HFA LI Frontal	0.540	0.656	0.813	0.930	0.606	0.103	0. 85	0.241
HFA LI Parietal	0.156	0.247	0.436	0.140	0.207	0.706	0. 85	0.203
HFA LI Temporal	0.188	0.856	0.552	0.804	0.790	0.736	0. 85	0.229
HMD LI Frontal	0.024	0.348	0.614	0.108	0.929	0.767	0. 85	0.398
HMD LI Parietal	0.894	0.914	0.326	0.982	0.206	0.110	0. 85	0.3401
HMD LI Temporal	0.171	0.611	0.664	0.356	0.250	0.796	0. 85	0.7555

Table 26 Heterogeneity (HG) lateralization index (LI) in gray matter (GM) as predictor for later rapid naming and phonologic performance
RAN: rapid automated naming at follow up, HND: Handedness, KBIT: non-verbal IQ, HFA and HMD: HG of FA and MD. The values represent significance level of variables' influence on HG. The last p-value corresponds to the F-statistic and is corrected for multiple comparisons. R^2 describes the models multiplied R^2.

ROI	RAN	CTOPP	Age	HND	KBIT	gender	p(F statistic)	R^2
HFA LI Frontal	0.982	0.652	0.907	0.770	0.685	0.077	0.85	0.226
HFA LI Parietal	0.488	0.711	0.310	0.824	0.524	0.960	0. 85	0.135
HFA LI Temporal	0.989	0.711	0.924	0.386	0.541	0.685	0. 85	0.226
HMD LI Frontal	0.308	0.303	0.187	0.375	0.219	0.201	0. 85	0.268
HMD LI Parietal	0.900	0.340	0.450	0.282	0.675	0.878	0. 85	0.221
HMD LI Temporal	0.433	0.746	0.537	0.513	0.387	0.500	0. 85	0.213

Table 27 Heterogeneity (HG) lateralization index (LI) in white matter (WM) as predictor for later rapid naming and phonologic performance
RAN: RAN at follow up, CTOPP: CTOPP at follow up HND: Handedness, KBIT: non-verbal IQ, HFA and HMD: HG of FA and MD. The values represent significance level of variables' influence on HG. The last p-value corresponds to the F-statistic and is corrected for multiple comparisons. R^2 describes the models multiplied R^2.

8 Bibliography

ADLER, W. T., PLATT, M. P., MEHLHORN, A. J., HAIGHT, J. L., CURRIER, T. A., ETCHEGARAY, M. A., GALABURDA, A. M. & ROSEN, G. D. 2013. Position of neocortical neurons transfected at different gestational ages with shRNA targeted against candidate dyslexia susceptibility genes. *PLoS One,* 8**,** e65179.

AVANTS, B. B., TUSTISON, N. J., SONG, G., COOK, P. A., KLEIN, A. & GEE, J. C. 2011. A reproducible evaluation of ANTs similarity metric performance in brain image registration. *Neuroimage,* 54**,** 2033-44.

BANFI, C., KOSCHUTNIG, K., MOLL, K., SCHULTE-KORNE, G., FINK, A. & LANDERL, K. 2019. White matter alterations and tract lateralization in children with dyslexia and isolated spelling deficits. *Hum Brain Mapp,* 40**,** 765-776.

BASSER, P. J., PAJEVIC, S., PIERPAOLI, C., DUDA, J. & ALDROUBI, A. 2000. In vivo fiber tractography using DT-MRI data. *Magn Reson Med,* 44**,** 625-32.

BASSER, P. J. & PIERPAOLI, C. 1996. Microstructural and physiological features of tissues elucidated by quantitative-diffusion-tensor MRI. *J Magn Reson B,* 111**,** 209-19.

BASSER, P. J. & PIERPAOLI, C. 1998. A simplified method to measure the diffusion tensor from seven MR images. *Magn Reson Med,* 39**,** 928-34.

BASSER, P. J. & PIERPAOLI, C. 2011. Microstructural and physiological features of tissues elucidated by quantitative-diffusion-tensor MRI. 1996. *J Magn Reson,* 213**,** 560-70.

BEAULIEU, C., YIP, E., LOW, P. B., MADLER, B., LEBEL, C. A., SIEGEL, L., MACKAY, A. L. & LAULE, C. 2020. Myelin Water Imaging Demonstrates Lower Brain Myelination in Children and Adolescents With Poor Reading Ability. *Front Hum Neurosci,* 14**,** 568395.

BECHSTEDT, S., LU, K. & BROUHARD, G. J. 2014. Doublecortin recognizes the longitudinal curvature of the microtubule end and lattice. *Curr Biol,* 24**,** 2366-75.

BOETS, B., OP DE BEECK, H. P., VANDERMOSTEN, M., SCOTT, S. K., GILLEBERT, C. R., MANTINI, D., BULTHE, J., SUNAERT, S., WOUTERS, J. & GHESQUIERE, P. 2013. Intact but less accessible phonetic representations in adults with dyslexia. *Science,* 342**,** 1251-4.

CAMPBELL, K. & GOTZ, M. 2002. Radial glia: multi-purpose cells for vertebrate brain development. *Trends Neurosci,* 25**,** 235-8.

CARRION-CASTILLO, A., FRANKE, B. & FISHER, S. E. 2013. Molecular genetics of dyslexia: an overview. *Dyslexia,* 19**,** 214-40.

CARROLL, J. M., MUNDY, I. R. & CUNNINGHAM, A. J. 2014. The roles of family history of dyslexia, language, speech production and phonological processing in predicting literacy progress. *Dev Sci,* 17**,** 727-42.

CARTER, J. C., LANHAM, D. C., CUTTING, L. E., CLEMENTS-STEPHENS, A. M., CHEN, X., HADZIPASIC, M., KIM, J., DENCKLA, M. B. & KAUFMANN, W. E. 2009. A dual DTI approach to analyzing white matter in children with dyslexia. *Psychiatry Res,* 172**,** 215-9.

CASANOVA, M. F., EL-BAZ, A. S., GIEDD, J., RUMSEY, J. M. & SWITALA, A. E. 2010. Increased white matter gyral depth in dyslexia: implications for corticocortical connectivity. *J Autism Dev Disord,* 40**,** 21-9.

CENTANNI, T. M., BOOKER, A. B., SLOAN, A. M., CHEN, F., MAHER, B. J., CARRAWAY, R. S., KHODAPARAST, N., RENNAKER, R., LOTURCO, J. J. & KILGARD, M. P. 2014. Knockdown of the dyslexia-associated gene Kiaa0319 impairs temporal responses to speech stimuli in rat primary auditory cortex. *Cereb Cortex,* 24**,** 1753-66.

CENTANNI, T. M., NORTON, E. S., OZERNOV-PALCHIK, O., PARK, A., BEACH, S. D., HALVERSON, K., GAAB, N. & GABRIELI, J. D. E. 2019. Disrupted left fusiform response to print in beginning kindergartners is associated with subsequent reading. *Neuroimage Clin,* 22**,** 101715.

CHANG, B. S., LY, J., APPIGNANI, B., BODELL, A., APSE, K. A., RAVENSCROFT, R. S., SHEEN, V. L., DOHERTY, M. J., HACKNEY, D. B., O'CONNOR, M.,

GALABURDA, A. M. & WALSH, C. A. 2005. Reading impairment in the neuronal migration disorder of periventricular nodular heterotopia. *Neurology,* 64**,** 799-803.
CLOWRY, G., MOLNAR, Z. & RAKIC, P. 2010. Renewed focus on the developing human neocortex. *J Anat,* 217**,** 276-88.
CUI, Z., XIA, Z., SU, M., SHU, H. & GONG, G. 2016. Disrupted white matter connectivity underlying developmental dyslexia: A machine learning approach. *Hum Brain Mapp,* 37**,** 1443-58.
CURRIER, T. A., ETCHEGARAY, M. A., HAIGHT, J. L., GALABURDA, A. M. & ROSEN, G. D. 2011. The effects of embryonic knockdown of the candidate dyslexia susceptibility gene homologue Dyx1c1 on the distribution of GABAergic neurons in the cerebral cortex. *Neuroscience,* 172**,** 535-46.
DALBY, M. A., ELBRO, C. & STODKILDE-JORGENSEN, H. 1998. Temporal lobe asymmetry and dyslexia: an in vivo study using MRI. *Brain Lang,* 62**,** 51-69.
DARKI, F., PEYRARD-JANVID, M., MATSSON, H., KERE, J. & KLINGBERG, T. 2012. Three dyslexia susceptibility genes, DYX1C1, DCDC2, and KIAA0319, affect temporo-parietal white matter structure. *Biol Psychiatry,* 72**,** 671-6.
DENCKLA, M. B. 1972. Color-naming defects in dyslexic boys. . *Cortex,* 8**,** 164-176.
DENCKLA, M. B. & RUDEL, R. G. 1976. Rapid "automatized" naming (R.A.N): dyslexia differentiated from other learning disabilities. *Neuropsychologia,* 14**,** 471-9.
DESIKAN, R. S., SEGONNE, F., FISCHL, B., QUINN, B. T., DICKERSON, B. C., BLACKER, D., BUCKNER, R. L., DALE, A. M., MAGUIRE, R. P., HYMAN, B. T., ALBERT, M. S. & KILLIANY, R. J. 2006. An automated labeling system for subdividing the human cerebral cortex on MRI scans into gyral based regions of interest. *Neuroimage,* 31**,** 968-80.
DEUEL, T. A., LIU, J. S., CORBO, J. C., YOO, S. Y., RORKE-ADAMS, L. B. & WALSH, C. A. 2006. Genetic interactions between doublecortin and doublecortin-like kinase in neuronal migration and axon outgrowth. *Neuron,* 49**,** 41-53.
DEUTSCH, G. K., DOUGHERTY, R. F., BAMMER, R., SIOK, W. T., GABRIELI, J. D. & WANDELL, B. 2005. Children's reading performance is correlated with white matter structure measured by diffusion tensor imaging. *Cortex,* 41**,** 354-63.
ECKERT, M. A., BERNINGER, V. W., VADEN, K. I., JR., GEBREGZIABHER, M. & TSU, L. 2016. Gray Matter Features of Reading Disability: A Combined Meta-Analytic and Direct Analysis Approach(1,2,3,4). *eNeuro,* 3.
EICHER, J. D., MONTGOMERY, A. M., AKSHOOMOFF, N., AMARAL, D. G., BLOSS, C. S., LIBIGER, O., SCHORK, N. J., DARST, B. F., CASEY, B. J., CHANG, L., ERNST, T., FRAZIER, J., KAUFMANN, W. E., KEATING, B., KENET, T., KENNEDY, D., MOSTOFSKY, S., MURRAY, S. S., SOWELL, E. R., BARTSCH, H., KUPERMAN, J. M., BROWN, T. T., HAGLER, D. J., JR., DALE, A. M., JERNIGAN, T. L., GRUEN, J. R. & PEDIATRIC IMAGING NEUROCOGNITION GENETICS, S. 2016. Dyslexia and language impairment associated genetic markers influence cortical thickness and white matter in typically developing children. *Brain Imaging Behav,* 10**,** 272-82.
EL-SADY, S., MOHAMMAD, S. A., ABOUALFOTOUH AHMED, K., KHATTAB, A. N., NASHAAT, N. H., ORABI, G. & ABDELRAOUF, E. R. 2020. Correlation between diffusion tensor imaging measures and the reading and cognitive performance of Arabic readers: dyslexic children perspective. *Neuroradiology,* 62**,** 525-531.
ELIEZ, S., RUMSEY, J. M., GIEDD, J. N., SCHMITT, J. E., PATWARDHAN, A. J. & REISS, A. L. 2000. Morphological alteration of temporal lobe gray matter in dyslexia: an MRI study. *J Child Psychol Psychiatry,* 41**,** 637-44.
EVANS, M. A., SHAW, D. & BELL, M. 2000. Home literacy activities and their influence on early literacy skills. *Can J Exp Psychol,* 54**,** 65-75.
FEDOROV, A., BEICHEL, R., KALPATHY-CRAMER, J., FINET, J., FILLION-ROBIN, J. C., PUJOL, S., BAUER, C., JENNINGS, D., FENNESSY, F., SONKA, M., BUATTI, J., AYLWARD, S., MILLER, J. V., PIEPER, S. & KIKINIS, R. 2012. 3D Slicer as an

image computing platform for the Quantitative Imaging Network. *Magn Reson Imaging,* 30**,** 1323-41.
FERNANDEZ, V. G., JURANEK, J., ROMANOWSKA-PAWLICZEK, A., STUEBING, K., WILLIAMS, V. J. & FLETCHER, J. M. 2015. White matter integrity of cerebellar-cortical tracts in reading impaired children: A probabilistic tractography study. *Brain Lang*.
FINN, E. S., SHEN, X., HOLAHAN, J. M., SCHEINOST, D., LACADIE, C., PAPADEMETRIS, X., SHAYWITZ, S. E., SHAYWITZ, B. A. & CONSTABLE, R. T. 2014. Disruption of functional networks in dyslexia: a whole-brain, data-driven analysis of connectivity. *Biol Psychiatry,* 76**,** 397-404.
FISCHL, B. 2012. FreeSurfer. *Neuroimage,* 62**,** 774-81.
FRYE, R. E., LIEDERMAN, J., HASAN, K. M., LINCOLN, A., MALMBERG, B., MCLEAN, J., 3RD & PAPANICOLAOU, A. 2011. Diffusion tensor quantification of the relations between microstructural and macrostructural indices of white matter and reading. *Hum Brain Mapp,* 32**,** 1220-35.
GALABURDA, A. & LIVINGSTONE, M. 1993. Evidence for a magnocellular defect in developmental dyslexia. *Ann N Y Acad Sci,* 682**,** 70-82.
GALABURDA, A. M. 1993a. Neuroanatomic basis of developmental dyslexia. *Neurol Clin,* 11**,** 161-73.
GALABURDA, A. M. 1993b. The planum temporale. *Arch Neurol,* 50**,** 457.
GALABURDA, A. M. & KEMPER, T. L. 1979. Cytoarchitectonic abnormalities in developmental dyslexia: a case study. *Ann Neurol,* 6**,** 94-100.
GALABURDA, A. M., LOTURCO, J., RAMUS, F., FITCH, R. H. & ROSEN, G. D. 2006. From genes to behavior in developmental dyslexia. *Nat Neurosci,* 9**,** 1213-7.
GALLAGHER, A., FRITH, U. & SNOWLING, M. J. 2000. Precursors of literacy delay among children at genetic risk of dyslexia. *J Child Psychol Psychiatry,* 41**,** 203-13.
GEBAUER, D., ENZINGER, C., KRONBICHLER, M., SCHURZ, M., REISHOFER, G., KOSCHUTNIG, K., KARGL, R., PURGSTALLER, C., FAZEKAS, F. & FINK, A. 2012. Distinct patterns of brain function in children with isolated spelling impairment: new insights. *Neuropsychologia,* 50**,** 1353-61.
GETMAN, G. N. 1985. A commentary on vision training. *J Learn Disabil,* 18**,** 505-12.
GOOCH, D., HULME, C., NASH, H. M. & SNOWLING, M. J. 2014. Comorbidities in preschool children at family risk of dyslexia. *J Child Psychol Psychiatry,* 55**,** 237-46.
GRIFFA, A., BAUMANN, P. S., THIRAN, J. P. & HAGMANN, P. 2013. Structural connectomics in brain diseases. *Neuroimage,* 80**,** 515-26.
GRIGORENKO, E. L. 2001. Developmental dyslexia: an update on genes, brains, and environments. *J Child Psychol Psychiatry,* 42**,** 91-125.
HAACKE, E. M. 1999. *Magnetic resonance imaging : physical principles and sequence design,* New York, Wiley.
HALLGREN, B. 1950. Specific dyslexia (congenital word-blindness); a clinical and genetic study. *Acta Psychiatr Neurol Suppl,* 65**,** 1-287.
HELENIUS, J., SOINNE, L., PERKIO, J., SALONEN, O., KANGASMAKI, A., KASTE, M., CARANO, R. A., ARONEN, H. J. & TATLISUMAK, T. 2002. Diffusion-weighted MR imaging in normal human brains in various age groups. *AJNR Am J Neuroradiol,* 23**,** 194-9.
HERMANN, K. 1959. *Reading disability; a medical study of word-blindness and related handicaps,* Copenhagen, Munksgaard.
HICKOK, G., HOUDE, J. & RONG, F. 2011. Sensorimotor integration in speech processing: computational basis and neural organization. *Neuron,* 69**,** 407-22.
HOEFT, F., MCCANDLISS, B. D., BLACK, J. M., GANTMAN, A., ZAKERANI, N., HULME, C., LYYTINEN, H., WHITFIELD-GABRIELI, S., GLOVER, G. H., REISS, A. L. & GABRIELI, J. D. 2011. Neural systems predicting long-term outcome in dyslexia. *Proc Natl Acad Sci U S A,* 108**,** 361-6.

HOLZ, M. H., S. R.; SACCO, A. 2000. Temperature-dependent selfdiffusion coefficients of water and six selected molecular liquids for calibration in accurate 1H NMR PFG measurements. *Physical Chemistry Chemical Physics,* 2**,** 4740-4742.

HOWARD, M. R. & HULIT, L. M. 1992. Response patterns to central auditory tests and the clinical evaluation of Language Fundamentals--Revised: a pilot study. *Percept Mot Skills,* 74**,** 120-2.

IM, K., PIENAAR, R., PALDINO, M. J., GAAB, N., GALABURDA, A. M. & GRANT, P. E. 2013. Quantification and discrimination of abnormal sulcal patterns in polymicrogyria. *Cereb Cortex,* 23**,** 3007-15.

IM, K., RASCHLE, N. M., SMITH, S. A., ELLEN GRANT, P. & GAAB, N. 2016. Atypical Sulcal Pattern in Children with Developmental Dyslexia and At-Risk Kindergarteners. *Cereb Cortex,* 26**,** 1138-1148.

JAGGER-RICKELS, A. C., KIBBY, M. Y. & CONSTANCE, J. M. 2018. Global gray matter morphometry differences between children with reading disability, ADHD, and comorbid reading disability/ADHD. *Brain Lang,* 185**,** 54-66.

JEDNOROG, K., GAWRON, N., MARCHEWKA, A., HEIM, S. & GRABOWSKA, A. 2014. Cognitive subtypes of dyslexia are characterized by distinct patterns of grey matter volume. *Brain Struct Funct,* 219**,** 1697-707.

JEZZARD, P., BARNETT, A. S. & PIERPAOLI, C. 1998. Characterization of and correction for eddy current artifacts in echo planar diffusion imaging. *Magn Reson Med,* 39**,** 801-12.

JOHNSON, H. 2018. BRAINSTools Package. https://github.com/BRAINSia/BRAINSTools.

KAUFMAN, A. S. A. K., N. L. 2014. Kaufman Brief Intelligence Test, Second Edition. *Encyclopedia of Special Education.* Yale University School of Medicine, New Haven, Connecticut.

KELLER, T. A. & JUST, M. A. 2009. Altering cortical connectivity: remediation-induced changes in the white matter of poor readers. *Neuron,* 64**,** 624-31.

KLINGBERG, T., HEDEHUS, M., TEMPLE, E., SALZ, T., GABRIELI, J. D., MOSELEY, M. E. & POLDRACK, R. A. 2000. Microstructure of temporo-parietal white matter as a basis for reading ability: evidence from diffusion tensor magnetic resonance imaging. *Neuron,* 25**,** 493-500.

KOIZUMI, H., TANAKA, T. & GLEESON, J. G. 2006. Doublecortin-like kinase functions with doublecortin to mediate fiber tract decussation and neuronal migration. *Neuron,* 49**,** 55-66.

KRAFNICK, A. J., FLOWERS, D. L., LUETJE, M. M., NAPOLIELLO, E. M. & EDEN, G. F. 2014. An investigation into the origin of anatomical differences in dyslexia. *J Neurosci,* 34**,** 901-8.

KRAFT, I., SCHREIBER, J., CAFIERO, R., METERE, R., SCHAADT, G., BRAUER, J., NEEF, N. E., MULLER, B., KIRSTEN, H., WILCKE, A., BOLTZE, J., FRIEDERICI, A. D. & SKEIDE, M. A. 2016. Predicting early signs of dyslexia at a preliterate age by combining behavioral assessment with structural MRI. *Neuroimage,* 143**,** 378-386.

LAMMINMAKI, S., MASSINEN, S., NOPOLA-HEMMI, J., KERE, J. & HARI, R. 2012. Human ROBO1 regulates interaural interaction in auditory pathways. *J Neurosci,* 32**,** 966-71.

LAYCOCK, S. K., WILKINSON, I. D., WALLIS, L. I., DARWENT, G., WONDERS, S. H., FAWCETT, A. J., GRIFFITHS, P. D. & NICOLSON, R. I. 2008. Cerebellar volume and cerebellar metabolic characteristics in adults with dyslexia. *Ann N Y Acad Sci,* 1145**,** 222-36.

LIEBENTHAL, E., SABRI, M., BEARDSLEY, S. A., MANGALATHU-ARUMANA, J. & DESAI, A. 2013. Neural dynamics of phonological processing in the dorsal auditory stream. *J Neurosci,* 33**,** 15414-24.

LINKERSDORFER, J., JURCOANE, A., LINDBERG, S., KAISER, J., HASSELHORN, M., FIEBACH, C. J. & LONNEMANN, J. 2015. The association between gray matter volume and reading proficiency: a longitudinal study of beginning readers. *J Cogn Neurosci,* 27**,** 308-18.

LIVINGSTONE, M. S., ROSEN, G. D., DRISLANE, F. W. & GALABURDA, A. M. 1991. Physiological and anatomical evidence for a magnocellular defect in developmental dyslexia. *Proc Natl Acad Sci U S A,* 88**,** 7943-7.

MA, Y., KOYAMA, M. S., MILHAM, M. P., CASTELLANOS, F. X., QUINN, B. T., PARDOE, H., WANG, X., KUZNIECKY, R., DEVINSKY, O., THESEN, T. & BLACKMON, K. 2015. Cortical thickness abnormalities associated with dyslexia, independent of remediation status. *Neuroimage Clin,* 7**,** 177-86.

MAAG, J. W. & REID, R. 2006. Depression among students with learning disabilities: assessing the risk. *J Learn Disabil,* 39**,** 3-10.

MARINO, C., SCIFO, P., DELLA ROSA, P. A., MASCHERETTI, S., FACOETTI, A., LORUSSO, M. L., GIORDA, R., CONSONNI, M., FALINI, A., MOLTENI, M., GRUEN, J. R. & PERANI, D. 2014. The DCDC2/intron 2 deletion and white matter disorganization: focus on developmental dyslexia. *Cortex,* 57**,** 227-43.

MCKINSTRY, R. C., MATHUR, A., MILLER, J. H., OZCAN, A., SNYDER, A. Z., SCHEFFT, G. L., ALMLI, C. R., SHIRAN, S. I., CONTURO, T. E. & NEIL, J. J. 2002. Radial organization of developing preterm human cerebral cortex revealed by non-invasive water diffusion anisotropy MRI. *Cereb Cortex,* 12**,** 1237-43.

MOLL, K., KUNZE, S., NEUHOFF, N., BRUDER, J. & SCHULTE-KORNE, G. 2014. Specific learning disorder: prevalence and gender differences. *PLoS One,* 9**,** e103537.

MOREAU, D., STONYER, J. E., MCKAY, N. S. & WALDIE, K. E. 2018. No evidence for systematic white matter correlates of dyslexia: An Activation Likelihood Estimation meta-analysis. *Brain Res,* 1683**,** 36-47.

MORENO-BRAVO, J. A., MARTINEZ-LOPEZ, J. E., MADRIGAL, M. P., KIM, M., MASTICK, G. S., LOPEZ-BENDITO, G., MARTINEZ, S. & PUELLES, E. 2016. Developmental guidance of the retroflex tract at its bending point involves Robo1-Slit2-mediated floor plate repulsion. *Brain Struct Funct,* 221**,** 665-78.

MORGAN, W. P. 1896. A Case of Congenital Word Blindness. *Br Med J,* 2**,** 1378.

MORI, S. 2007. *Introduction to Diffusion Tensor Imaging,* Elsevier Science.

MUKHOPADHYAY, M., PELKA, P., DESOUSA, D., KABLAR, B., SCHINDLER, A., RUDNICKI, M. A. & CAMPOS, A. R. 2002. Cloning, genomic organization and expression pattern of a novel Drosophila gene, the disco-interacting protein 2 (dip2), and its murine homolog. *Gene,* 293**,** 59-65.

NELSON, J. M. & LIEBEL, S. W. 2018. Socially Desirable Responding and College Students with Dyslexia: Implications for the Assessment of Anxiety and Depression. *Dyslexia,* 24**,** 44-58.

NOLTE, J. 2009. *The human brain : an introduction to its functional anatomy,* Philadelphia, PA, Mosby/Elsevier.

ODEGARD, T. N., FARRIS, E. A., RING, J., MCCOLL, R. & BLACK, J. 2009. Brain connectivity in non-reading impaired children and children diagnosed with developmental dyslexia. *Neuropsychologia,* 47**,** 1972-7.

OLULADE, O. A., NAPOLIELLO, E. M. & EDEN, G. F. 2013. Abnormal visual motion processing is not a cause of dyslexia. *Neuron,* 79**,** 180-90.

PANAGIOTAKI, E., SCHNEIDER, T., SIOW, B., HALL, M. G., LYTHGOE, M. F. & ALEXANDER, D. C. 2012. Compartment models of the diffusion MR signal in brain white matter: a taxonomy and comparison. *Neuroimage,* 59**,** 2241-54.

PARTANEN, M., KIM, D. H. C., RAUSCHER, A., SIEGEL, L. S. & GIASCHI, D. E. 2020. White matter but not grey matter predicts change in reading skills after intervention. *Dyslexia*.

PASTERNAK, O., SOCHEN, N., GUR, Y., INTRATOR, N. & ASSAF, Y. 2009. Free water elimination and mapping from diffusion MRI. *Magn Reson Med,* 62**,** 717-30.

PENNINGTON, B. F. & LEFLY, D. L. 2001. Early reading development in children at family risk for dyslexia. *Child Dev,* 72**,** 816-33.

PERNET, C. R., POLINE, J. B., DEMONET, J. F. & ROUSSELET, G. A. 2009. Brain classification reveals the right cerebellum as the best biomarker of dyslexia. *BMC Neurosci,* 10**,** 67.

PHAN, T. V., SIMA, D. M., BEELEN, C., VANDERAUWERA, J., SMEETS, D. & VANDERMOSTEN, M. 2018. Evaluation of methods for volumetric analysis of pediatric brain data: The childmetrix pipeline versus adult-based approaches. *Neuroimage Clin,* 19**,** 734-744.

POELMANS, G., ENGELEN, J. J., VAN LENT-ALBRECHTS, J., SMEETS, H. J., SCHOENMAKERS, E., FRANKE, B., BUITELAAR, J. K., WUISMAN-FRERKER, M., ERENS, W., STEYAERT, J. & SCHRANDER-STUMPEL, C. 2009. Identification of novel dyslexia candidate genes through the analysis of a chromosomal deletion. *Am J Med Genet B Neuropsychiatr Genet,* 150B**,** 140-7.

QUINN, J. M. & WAGNER, R. K. 2015. Gender Differences in Reading Impairment and in the Identification of Impaired Readers: Results From a Large-Scale Study of At-Risk Readers. *J Learn Disabil,* 48**,** 433-45.

R_DEVELOPMENT_CORE_TEAM 2008. *R: A language and environment for statistical computing.* , R Foundation for Statistical Computing, Vienna, Austria. .

RAMUS, F. & SZENKOVITS, G. 2008. What phonological deficit? *Q J Exp Psychol (Hove),* 61**,** 129-41.

RASCHLE, N. M., CHANG, M. & GAAB, N. 2011. Structural brain alterations associated with dyslexia predate reading onset. *Neuroimage,* 57**,** 742-9.

RASCHLE, N. M., STERING, P. L., MEISSNER, S. N. & GAAB, N. 2014. Altered neuronal response during rapid auditory processing and its relation to phonological processing in prereading children at familial risk for dyslexia. *Cereb Cortex,* 24**,** 2489-501.

RASCHLE, N. M., ZUK, J. & GAAB, N. 2012. Functional characteristics of developmental dyslexia in left-hemispheric posterior brain regions predate reading onset. *Proc Natl Acad Sci U S A,* 109**,** 2156-61.

RASHOTTE, R. W. J. T. C. 1999. Comprehensive test of phonological processing. *(Austin, TX: Pro-ed)*.

RATHI, Y., PASTERNAK, O., SAVADJIEV, P., MICHAILOVICH, O., BOUIX, S., KUBICKI, M., WESTIN, C. F., MAKRIS, N. & SHENTON, M. E. 2014. Gray matter alterations in early aging: a diffusion magnetic resonance imaging study. *Hum Brain Mapp,* 35**,** 3841-56.

RENDALL, A. R., TARKAR, A., CONTRERAS-MORA, H. M., LOTURCO, J. J. & FITCH, R. H. 2015. Deficits in learning and memory in mice with a mutation of the candidate dyslexia susceptibility gene Dyx1c1. *Brain Lang*.

RICHARDS, T., STEVENSON, J., CROUCH, J., JOHNSON, L. C., MARAVILLA, K., STOCK, P., ABBOTT, R. & BERNINGER, V. 2008. Tract-based spatial statistics of diffusion tensor imaging in adults with dyslexia. *AJNR Am J Neuroradiol,* 29**,** 1134-9.

RICHARDS, T. L., BERNINGER, V. W., YAGLE, K. J., ABBOTT, R. D. & PETERSON, D. J. 2017. Changes in DTI Diffusivity and fMRI Connectivity Cluster Coefficients for Students with and without Specific Learning Disabilities In Written Language: Brain's Response to Writing Instruction. *J Nat Sci,* 3.

RICHARDS, T. L., GRABOWSKI, T. J., BOORD, P., YAGLE, K., ASKREN, M., MESTRE, Z., ROBINSON, P., WELKER, O., GULLIFORD, D., NAGY, W. & BERNINGER, V. 2015. Contrasting brain patterns of writing-related DTI parameters, fMRI connectivity, and DTI-fMRI connectivity correlations in children with and without dysgraphia or dyslexia. *Neuroimage Clin,* 8**,** 408-21.

RICHARDSON, F. M., RAMSDEN, S., ELLIS, C., BURNETT, S., MEGNIN, O., CATMUR, C., SCHOFIELD, T. M., LEFF, A. P. & PRICE, C. J. 2011. Auditory short-term memory capacity correlates with gray matter density in the left posterior STS in cognitively normal and dyslexic adults. *J Cogn Neurosci,* 23**,** 3746-56.

RICHLAN, F., KRONBICHLER, M. & WIMMER, H. 2013. Structural abnormalities in the dyslexic brain: a meta-analysis of voxel-based morphometry studies. *Hum Brain Mapp,* 34**,** 3055-65.

RIMRODT, S. L., PETERSON, D. J., DENCKLA, M. B., KAUFMANN, W. E. & CUTTING, L. E. 2010. White matter microstructural differences linked to left perisylvian language network in children with dyslexia. *Cortex,* 46**,** 739-49.

ROALF, D. R., QUARMLEY, M., ELLIOTT, M. A., SATTERTHWAITE, T. D., VANDEKAR, S. N., RUPAREL, K., GENNATAS, E. D., CALKINS, M. E., MOORE, T. M., HOPSON, R., PRABHAKARAN, K., JACKSON, C. T., VERMA, R., HAKONARSON, H., GUR, R. C. & GUR, R. E. 2016. The impact of quality assurance assessment on diffusion tensor imaging outcomes in a large-scale population-based cohort. *Neuroimage,* 125**,** 903-19.

ROBERTS, J., JURGENS, J. & BURCHINAL, M. 2005. The role of home literacy practices in preschool children's language and emergent literacy skills. *J Speech Lang Hear Res,* 48**,** 345-59.

ROHDE, G. K., BARNETT, A. S., BASSER, P. J., MARENCO, S. & PIERPAOLI, C. 2004. Comprehensive approach for correction of motion and distortion in diffusion-weighted MRI. *Magn Reson Med,* 51**,** 103-14.

SAYGIN, Z. M., NORTON, E. S., OSHER, D. E., BEACH, S. D., CYR, A. B., OZERNOV-PALCHIK, O., YENDIKI, A., FISCHL, B., GAAB, N. & GABRIELI, J. D. 2013. Tracking the roots of reading ability: white matter volume and integrity correlate with phonological awareness in prereading and early-reading kindergarten children. *J Neurosci,* 33**,** 13251-8.

SCHULTE-KORNE, G., DEIMEL, W. & REMSCHMIDT, H. 2003. [Practice in spelling in remedial groups--results of an evaluation study in secondary education]. *Z Kinder Jugendpsychiatr Psychother,* 31**,** 85-98.

SCHULTE-KORNE, G., WARNKE, A. & REMSCHMIDT, H. 2006. [Genetics of dyslexia]. *Z Kinder Jugendpsychiatr Psychother,* 34**,** 435-44.

SEITZ, J., RATHI, Y., LYALL, A., PASTERNAK, O., DEL RE, E. C., NIZNIKIEWICZ, M., NESTOR, P., SEIDMAN, L. J., PETRYSHEN, T. L., MESHOLAM-GATELY, R. I., WOJCIK, J., MCCARLEY, R. W., SHENTON, M. E., KOERTE, I. K. & KUBICKI, M. 2018. Alteration of gray matter microstructure in schizophrenia. *Brain Imaging Behav,* 12**,** 54-63.

SELEMON, L. D. & GOLDMAN-RAKIC, P. S. 1999. The reduced neuropil hypothesis: a circuit based model of schizophrenia. *Biol Psychiatry,* 45**,** 17-25.

SHAYWITZ, S. E., SHAYWITZ, B. A., PUGH, K. R., FULBRIGHT, R. K., CONSTABLE, R. T., MENCL, W. E., SHANKWEILER, D. P., LIBERMAN, A. M., SKUDLARSKI, P., FLETCHER, J. M., KATZ, L., MARCHIONE, K. E., LACADIE, C., GATENBY, C. & GORE, J. C. 1998. Functional disruption in the organization of the brain for reading in dyslexia. *Proc Natl Acad Sci U S A,* 95**,** 2636-41.

SIGURDARDOTTIR, H. M., IVARSSON, E., KRISTINSDOTTIR, K. & KRISTJANSSON, A. 2015. Impaired recognition of faces and objects in dyslexia: Evidence for ventral stream dysfunction? *Neuropsychology,* 29**,** 739-50.

SMITH, S. D., KIMBERLING, W. J., PENNINGTON, B. F. & LUBS, H. A. 1983. Specific reading disability: identification of an inherited form through linkage analysis. *Science,* 219**,** 1345-7.

SONG, S. K., SUN, S. W., RAMSBOTTOM, M. J., CHANG, C., RUSSELL, J. & CROSS, A. H. 2002. Dysmyelination revealed through MRI as increased radial (but unchanged axial) diffusion of water. *Neuroimage,* 17**,** 1429-36.

STANOVICH, K. 1996. Toward a More Inclusive Definition of Dyslexia. *Dyslexia,* 2**,** 154-166.

STEINBRINK, C., VOGT, K., KASTRUP, A., MULLER, H. P., JUENGLING, F. D., KASSUBEK, J. & RIECKER, A. 2008. The contribution of white and gray matter differences to developmental dyslexia: insights from DTI and VBM at 3.0 T. *Neuropsychologia,* 46**,** 3170-8.

STORCH, S. A. & WHITEHURST, G. J. 2001. The role of family and home in the literacy development of children from low-income backgrounds. *New Dir Child Adolesc Dev***,** 53-71; discussion 91-8.

STREINER, D. L. & NORMAN, G. R. 2011. Correction for multiple testing: is there a resolution? *Chest,* 140**,** 16-18.

SU, M., ZHAO, J., THIEBAUT DE SCHOTTEN, M., ZHOU, W., GONG, G., RAMUS, F. & SHU, H. 2018. Alterations in white matter pathways underlying phonological and morphological processing in Chinese developmental dyslexia. *Dev Cogn Neurosci,* 31**,** 11-19.

SUN, X., SONG, S., LIANG, X., XIE, Y., ZHAO, C., ZHANG, Y., SHU, H. & GONG, G. 2017. ROBO1 polymorphisms, callosal connectivity, and reading skills. *Hum Brain Mapp,* 38**,** 2616-2626.

TAMBOER, P., SCHOLTE, H. S. & VORST, H. C. 2015. Dyslexia and voxel-based morphometry: correlations between five behavioural measures of dyslexia and gray and white matter volumes. *Ann Dyslexia,* 65**,** 121-41.

TAMBOER, P., VORST, H. C. M., GHEBREAB, S. & SCHOLTE, H. S. 2016. Machine learning and dyslexia: Classification of individual structural neuro-imaging scans of students with and without dyslexia. *Neuroimage Clin,* 11**,** 508-514.

TAMMIMIES, K., VITEZIC, M., MATSSON, H., LE GUYADER, S., BURGLIN, T. R., OHMAN, T., STROMBLAD, S., DAUB, C. O., NYMAN, T. A., KERE, J. & TAPIA-PAEZ, I. 2013. Molecular networks of DYX1C1 gene show connection to neuronal migration genes and cytoskeletal proteins. *Biol Psychiatry,* 73**,** 583-90.

TAMNES, C. K., OSTBY, Y., FJELL, A. M., WESTLYE, L. T., DUE-TONNESSEN, P. & WALHOVD, K. B. 2010. Brain maturation in adolescence and young adulthood: regional age-related changes in cortical thickness and white matter volume and microstructure. *Cereb Cortex,* 20**,** 534-48.

THE MATHWORKS, I. 2015. MATLAB and Statistics Toolbox Release. 8.5.0 (R2015a) ed. Natick, Massachusetts, United States.

TORGENSEN, J., WAGNER, R. & RASHOTTE, C. 1999. Test of Word Reading Interesting (TOWRE). *London: Psychological Corporation*.

TRAN, C., WIGG, K. G., ZHANG, K., CATE-CARTER, T. D., KERR, E., FIELD, L. L., KAPLAN, B. J., LOVETT, M. W. & BARR, C. L. 2014. Association of the ROBO1 gene with reading disabilities in a family-based analysis. *Genes Brain Behav,* 13**,** 430-8.

VAN OERS, C., GOLDBERG, N., FIORIN, G., VAN DEN HEUVEL, M. P., KAPPELLE, L. J. & WIJNEN, F. N. K. 2018. No evidence for cerebellar abnormality in adults with developmental dyslexia. *Exp Brain Res,* 236**,** 2991-3001.

VANDER STAPPEN, C., DRICOT, L. & VAN REYBROECK, M. 2020. RAN training in dyslexia: Behavioral and brain correlates. *Neuropsychologia,* 146**,** 107566.

VANDERAUWERA, J., VAN SETTEN, E. R. H., MAURITS, N. M. & MAASSEN, B. A. M. 2019. The interplay of socio-economic status represented by paternal educational level, white matter structure and reading. *PLoS One,* 14**,** e0215560.

VANDERAUWERA, J., WOUTERS, J., VANDERMOSTEN, M. & GHESQUIERE, P. 2017. Early dynamics of white matter deficits in children developing dyslexia. *Dev Cogn Neurosci,* 27**,** 69-77.

VANDERMOSTEN, M., BOETS, B., POELMANS, H., SUNAERT, S., WOUTERS, J. & GHESQUIERE, P. 2012a. A tractography study in dyslexia: neuroanatomic correlates of orthographic, phonological and speech processing. *Brain,* 135**,** 935-48.

VANDERMOSTEN, M., BOETS, B., WOUTERS, J. & GHESQUIERE, P. 2012b. A qualitative and quantitative review of diffusion tensor imaging studies in reading and dyslexia. *wNeurosci Biobehav Rev,* 36**,** 1532-52.

VANDERMOSTEN, M., POELMANS, H., SUNAERT, S., GHESQUIERE, P. & WOUTERS, J. 2013. White matter lateralization and interhemispheric coherence to auditory modulations in normal reading and dyslexic adults. *Neuropsychologia,* 51**,** 2087-99.

VANDERMOSTEN, M., VANDERAUWERA, J., THEYS, C., DE VOS, A., VANVOOREN, S., SUNAERT, S., WOUTERS, J. & GHESQUIERE, P. 2015. A DTI tractography study in pre-readers at risk for dyslexia. *Dev Cogn Neurosci,* 14**,** 8-15.

VELAYOS-BAEZA, A., TOMA, C., DA ROZA, S., PARACCHINI, S. & MONACO, A. P. 2007. Alternative splicing in the dyslexia-associated gene KIAA0319. *Mamm Genome,* 18**,** 627-34.

VELLUTINO, F. R. 1979. *Dyslexia : theory and research,* Cambridge, Mass., MIT Press.

VELLUTINO, F. R. 1987. Dyslexia. *Sci Am,* 256**,** 34-41.

VINCKENBOSCH, E., ROBICHON, F. & ELIEZ, S. 2005. Gray matter alteration in dyslexia: converging evidence from volumetric and voxel-by-voxel MRI analyses. *Neuropsychologia,* 43**,** 324-31.

WALHOVD, K. B., FJELL, A. M., GIEDD, J., DALE, A. M. & BROWN, T. T. 2017. Through Thick and Thin: a Need to Reconcile Contradictory Results on Trajectories in Human Cortical Development. *Cereb Cortex,* 27**,** 1472-1481.

WANG, H. S., WANG, N. Y. & YEH, F. C. 2019. Specifying the diffusion MRI connectome in Chinese-speaking children with developmental dyslexia and auditory processing deficits. *Pediatr Neonatol,* 60**,** 297-304.

WANG, Y., PARAMASIVAM, M., THOMAS, A., BAI, J., KAMINEN-AHOLA, N., KERE, J., VOSKUIL, J., ROSEN, G. D., GALABURDA, A. M. & LOTURCO, J. J. 2006. DYX1C1 functions in neuronal migration in developing neocortex. *Neuroscience,* 143**,** 515-22.

WELCOME, S. E., CHIARELLO, C., THOMPSON, P. M. & SOWELL, E. R. 2011. Reading skill is related to individual differences in brain structure in college students. *Hum Brain Mapp,* 32**,** 1194-205.

WHO 2014. *ICD-10-GM 2015 Systematisches Verzeichnis: Internationale statistische Klassifikation der Krankheiten und verwandter Gesundheitsprobleme* Deutscher Ärzte-Verlag.

WINKLER, A. M., KOCHUNOV, P., BLANGERO, J., ALMASY, L., ZILLES, K., FOX, P. T., DUGGIRALA, R. & GLAHN, D. C. 2010. Cortical thickness or grey matter volume? The importance of selecting the phenotype for imaging genetics studies. *Neuroimage,* 53**,** 1135-46.

WOLF, M. & BOWERS, P. 1999. The Double-Deficit Hypothesis for the Developmental Dyslexias. *Journal of Educational Psychology,* 91**,** 415-438.

WOLF, M. & BOWERS, P. G. 2000. Naming-speed processes and developmental reading disabilities: an introduction to the special issue on the double-deficit hypothesis. *J Learn Disabil,* 33**,** 322-4.

WOLF, M. D., MB 2005. RAN/RAS: Rapid automatized naming and rapid alternating stimulus tests. Austin, TX: Pro-ed Inc.

WOODCOCK, R. 1998. *Woodcock Reading Mastery Test - Revised.* , Minneapolis, MN: NCS Pearson Inc. .

XIA, Z., HOEFT, F., ZHANG, L. & SHU, H. 2016. Neuroanatomical anomalies of dyslexia: Disambiguating the effects of disorder, performance, and maturation. *Neuropsychologia,* 81**,** 68-78.

YEATMAN, J. D., DOUGHERTY, R. F., RYKHLEVSKAIA, E., SHERBONDY, A. J., DEUTSCH, G. K., WANDELL, B. A. & BEN-SHACHAR, M. 2011. Anatomical properties of the arcuate fasciculus predict phonological and reading skills in children. *J Cogn Neurosci,* 23**,** 3304-17.

ZHUANG, J., HRABE, J., KANGARLU, A., XU, D., BANSAL, R., BRANCH, C. A. & PETERSON, B. S. 2006. Correction of eddy-current distortions in diffusion tensor images using the known directions and strengths of diffusion gradients. *J Magn Reson Imaging,* 24**,** 1188-93.

ZUK, J., DUNSTAN, J., NORTON, E., YU, X., OZERNOV-PALCHIK, O., WANG, Y., HOGAN, T. P., GABRIELI, J. D. E. & GAAB, N. 2020. Multifactorial pathways facilitate resilience among kindergarteners at risk for dyslexia: A longitudinal behavioral and neuroimaging study. *Dev Sci***,** e12983.

9. Acknowledgements

This work depended on the effort and time contributions of the numerous participants and their families, who have supported the development of neuroscience.

I am grateful for the support received from Prof. Dr. med. Inga Koerte, Professor for Neurobiological Research in Child and Adolescent Psychiatry, *Klinik und Poliklinik für Kinder- und Jugendpsychiatrie, Psychosomatik und Psychotherapie*, Munich, Germany. Professor Koerte kindly considered my application, thus offering a formative and highly educative year of research in the United States. In addition, Professor Koerte not only showed me the quality of good scientific practice in a very patient way but also inspired creative thinking and endurance when trying to achieve my aims.

I would like to express my gratitude to Professor Martha E. Shenton, head of the Psychiatry Neuroimaging Laboratory, Harvard Medical School for the opportunity to spend a year in her laboratory and gather the material for this work. I want to thank her further for the time offered to thoroughly discuss my work, her kind advice, and the hospitality I received at the laboratory.

Moreover, I want to thank Sylvain Bouix, Ofer Pasternak and Yogesh Rathi, Associate Professors at the Laboratory of Mathematics in Imaging, Harvard Medical School, for their advice and the opportunity to learn the technical aspects of high-quality imaging processing, free-water correction and investigation into HG measures.

Next, I express my gratitude to Professor Nadine Gaab, head of the Gaab Laboratory, Boston Children's Hospital, Harvard Medical School. The great collaboration with her group provided access to the BOLD study data. I appreciate Professor Gaab's valuable support and numerous insights into the neurobehavioral aspects of reading.

Then, because of the support offered by Dr. rer. biol. hum. Sarolta Bakos regarding the additional processing of 31 time point data sets, the number of participants included in the analysis could be increased. Moreover, I want to thank Dr. med. Johanna Seitz-Holland for the numerous discussions of statistical analysis.

Last but not least, I thank my Grandparents for their time dedicated to my development, my Parents for teaching me to be thorough in whatever I do, my sister Maria for sharing her opinion on this work and my brother Wojciech for constantly reminding me of responsibility. When writing this work on reading I express my gratitude to Melita Kubalewska and the dear BU for sharing this ability with me. Finally,

Last paragraph in Polish language:

Na koncu, ale i honorowym miejscu chciałbym też podziękować Dziadkom za czas poświęcony mojemu rozwojowi (już nie o.m.c.), Rodzicom za szkołę bycia sumiennym, Marii za komentowanie tej pracy i Wojtkowi za ciągłe przypominanie o odpowiedzialności. Pisząc pracę o konstrukcie jakim jest czytanie dziękuję też Melicie Kubalewskiej i oczywiście drogiej BU za podzielenie się tą umiejętnością.